Neutrino Oscillations and the MSW Effect

S. T. Petcov

SISSA/INFN, Trieste, Italy,
IPMU, University of Tokyo, Tokyo, Japan and
INRNE, Bulgarian Academy of Sciences, Sofia, Bulgaria

Le Neutrino dans tous ses e'tats
Journe'e Jacques Bouchez
November 19, 2010, Saclay

Jacques was a highly valuable member of our international Neutrino Physics Family. It was always useful and interesting to discuss with him - he had the gift of looking at a problem from completely unexpected angle and proposing original solutions. His human warmth made the communication with him pleasant and memorable. The memory of Jacques is vivid and alive.

Jacques and neutrinos: Bugey; NOMAD; K2K; beta beams; neutrino factories; megaton detectors (Frejus; UNO).

First work on neutrinos (to my knowledge): 1986.

Z. Phys. C – Particles and Fields 32, 499–511 (1986)

Zeitschrift für Physik C Particles and Fields

Matter Effects for Solar Neutrino Oscillations

J. Bouchez[1], M. Cribier[1], W. Hampel[2], J. Rich[1], M. Spiro[1], D. Vignaud[1]

[1] DPhPE, CEN Saclay, F-91191 Gif-sur-Yvette, France
[2] Max Planck Institut für Kernphysik, D-6900 Heidelberg, Federal Republic of Germany

Received 7 May 1986; in revised form 16 June 1986

Abstract. Possible solar neutrino oscillations are reviewed in the two-neutrino case taking into account the effect of coherent forward scattering when neutrinos travel through the sun and earth. As recently pointed out by Mikheyev and Smirnov this effect can induce a large suppression of the solar ν_e flux for values of Δm^2 around $10^{-4}-10^{-8}\,\mathrm{eV}^2$ even for small values of the mixing angle. It also may cause substantial modifications of the solar neutrino spectrum shape. All this may be used for determining Δm^2 and $\sin^2 2\theta$ in a large domain from the experimental results of the chlorine, gallium, indium and heavy water detectors.

1. Introduction

As was first suggested by Pontecorvo [1], if neutrinos are massive and if there is nonconservation of the lepton family number, the mass eigenstates ν_1 and ν_2 (of masses m_1 and m_2) may differ from ν_e and ν_μ, leading to flavor oscillations when neutrinos propagate in vacuum. This oscillation is due to the phase mismatch φ_v between the ν_1 and ν_2 components (energies E_1 and E_2) for a given momentum p:

$$d\varphi_v/dt = E_1 - E_2 = \sqrt{p^2+m_1^2} - \sqrt{p^2+m_2^2}$$
$$\simeq (m_1^2 - m_2^2)/2p \quad \text{if } p \gg m_i.$$

(Except where stated otherwise we have set $\hbar = c = 1$). The oscillation hypothesis has been used among others to explain the discrepancy between the solar neutrino signal observed with the chlorine experiment and that predicted by the standard solar model (SSM) [2]. Such calculations concerning vacuum oscillations for solar neutrino experiments have been performed by Hampel [3] following the work by Barger et al. [4].

When neutrinos propagate in matter, Wolfenstein showed [5] that a new phase mismatch between ν_e and ν_μ components appears due to the difference in forward elastic scattering of ν_e and ν_μ on electrons (see Fig. 1), since the W exchange graph shown on Fig. 1c is operative only for ν_e. For neutrinos the phase mismatch φ_m obeys [5]:

$$d\varphi_m/dt = k(x) = \sqrt{2}\cdot G\cdot N(x)$$

where $x = ct$ and where $N(x)$ is the electron density in cm^{-3} and G is the Fermi coupling constant. The net effect of this new phase is that the propagation eigenstates in matter are no longer the mass eigenstates ν_1 and ν_2, therefore oscillation parameters in matter differ from those in vacuum. This formalism was extended to three neutrino oscillations by Barger et al. [6]. More recently Mikheyev and Smirnov [7] showed that the difference might introduce dramatic effects for solar neutrinos, which may lead to a very strong suppression of the ν_e flux measured on earth, even if the vacuum mixing angle is small.

In this paper we develop the formalism of two-neutrino oscillations in matter in a way exhibiting the possible approximations and their limits. We then apply it to the solar neutrino case and demonstrate the consequences for the chlorine experiment [2], the forthcoming gallium experiment [3, 8] and possible future indium [9] or heavy water experiments [10]. The results of Mikheyev and Smirnov are confirmed and completed. We explain in particular how solar neutrino experiments can provide unambiguous information about Δm^2 (where $\Delta m^2 = m_1^2 - m_2^2$) and $\sin^2 2\theta$ in a large region of the corresponding plane by using the absolute experimental rates and the shape of the solar neutrino energy distribution. Preliminary results have been given elsewhere [11]. Several results on the same topic appeared very recently [12–14]. Our approach to the solar neutrino problem is different and, we think, more general.

2. Formalism for Oscillations in Matter

Firstly we recall briefly the formalism for vacuum oscillations. We then present the formalism for oscillations in matter and give a geometrical approach of the phenomenon.

Compellings Evidence for ν−Oscillations

$-\nu_{\text{atm}}$: SK UP-DOWN ASYMMETRY

θ_Z-, $L/E-$ **dependences of $\mu-$like events**

Dominant $\nu_\mu \longrightarrow \nu_\tau$ K2K, MINOS; CNGS (OPERA)

$-\nu_\odot$: **Homestake, Kamiokande, SAGE, GALLEX/GNO**
Super-Kamiokande, SNO, BOREXINO; KamLAND

Dominant $\nu_e \longrightarrow \nu_{\mu,\tau}$ **BOREXINO; possibly LowNu**

− LSND: **Dominant** $\bar{\nu}_\mu \longrightarrow \bar{\nu}_e$;

MiniBOONE 2010: $\nu_\mu \longrightarrow \nu_e$ incompatible, $\bar{\nu}_\mu \longrightarrow \bar{\nu}_e$ compatible (!?)

$$\nu_{l\text{L}} = \sum_{j=1} U_{lj}\, \nu_{j\text{L}} \qquad l = e, \mu, \tau.$$

B. Pontecorvo, 1957; 1958; 1967;
Z. Maki, M. Nakagawa, S. Sakata, 1962;

2001− Remarkable progress in the studies of $\nu-$ mixing and oscillations

- June, 2001: SNO CC data + SK data $\rightarrow$ $\nu_{\mu,\tau}$ and/or $\bar{\nu}_{\mu,\tau}$ in $\Phi_E(\nu_\odot)$

- April, 2002: SNO NC data $\rightarrow$ evidence for $\nu_{\mu,\tau}$ and/or $\bar{\nu}_{\mu,\tau}$ in $\Phi_E(\nu_\odot)$ strengthen

- December, 2002: KamLAND
  - **First compelling evidence for $\nu-$oscillations in an experiment with terrestrial ν's**
  - **Evidence for ν_e-mixing in vacuum**
  - **$\nu_\odot$: LMA solution (CPT)**
  - **KamLAND "massacre":**

  VO, QVO, LOW, SMA MSW, RSFP, FCNC, WEPV, LIV,...

- September, 2003: SNO salt phase data, $\Phi_B(\nu_\odot)$ - higher precision

- 2004: KamLAND, e^+-spectrum; K2K, $\nu_\mu-$spectrum SK, L/E; SNO

Solar Neutrinos

$$4p \rightarrow {}^4He + 2e^+ + 2\nu_e.$$

- pp neutrinos, $E \leq 0.420$ MeV, $\bar{E} = 0.265$ MeV,
- ${}^7Be$ neutrinos, E=0.862 MeV (89.7% of the flux), 0.384 MeV (10.3%) ,
- ${}^8B$ neutrinos, $E \leq 14.40$ MeV, $\bar{E} = 6.71$ MeV,
- pep neutrinos, E=1.442 MeV,
- of ${}^{13}N$, $E \leq 1.199$ MeV, $\bar{E} = 0.707$ MeV,
- of ${}^{15}O$, $E \leq 1.732$ MeV, $\bar{E} = 0.997$ MeV.

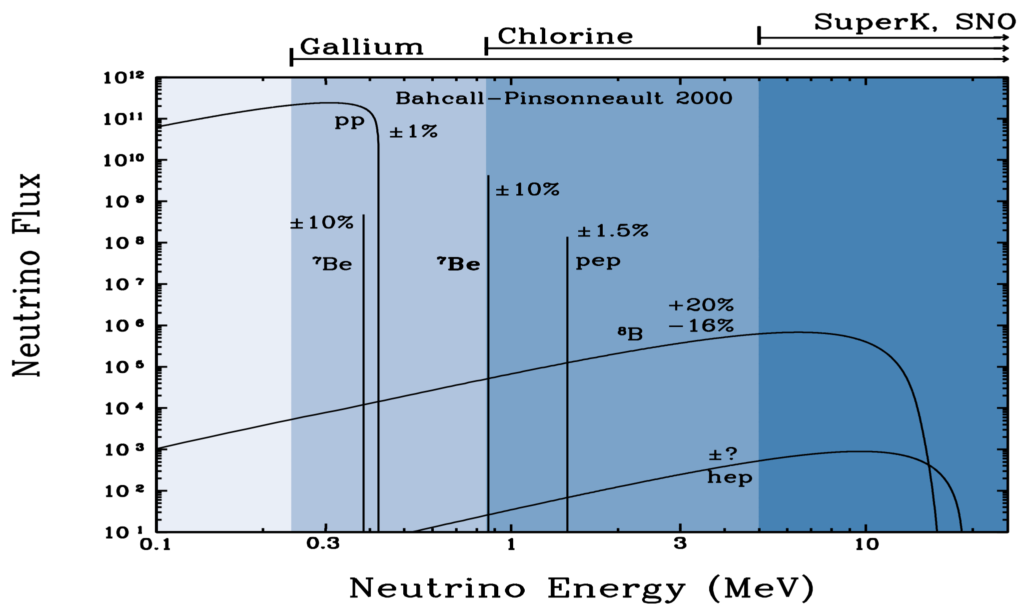

Figure 2: Differential Standard Solar Model neutrino fluxes [14].

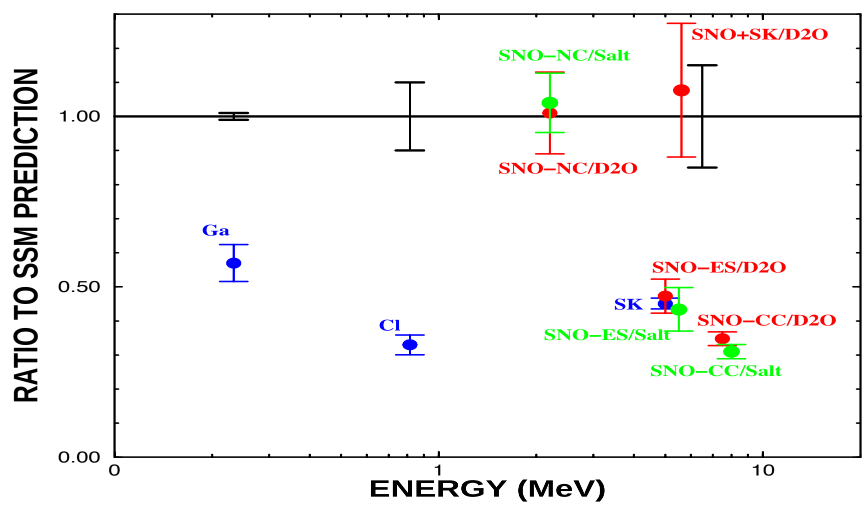

Figure 3: Comparison of measurements to Standard Solar Model predictions.

[tb] Results from radiochemical solar-neutrino experiments. The predictions of a recent standard solar model BPS08(GS) are also shown. The first and the second errors in the experimental results are the statistical and systematic errors, respectively. SNU (Solar Neutrino Unit) is defined as 10^{-36} neutrino captures per atom per second.

Ref.	^{37}Cl$\rightarrow$^{37}Ar	^{71}Ga$\rightarrow$^{71}Ge	
		(SNU)	(SNU)
Homestake	(Cleveland98)	$2.56 \pm 0.16 \pm 0.16$	—
GALLEX	(Hampel99)	—	$77.5 \pm 6.2^{+4.3}_{-4.7}$
GNO	(Altmann05)	—	$62.9^{+5.5}_{-5.3} \pm 2.5$
GNO+GALLEX	(Altmann05)	—	$69.3 \pm 4.1 \pm 3.6$
SAGE	(SAGE09)	—	$65.4^{+3.1+2.6}_{-3.0-2.8}$
SSM [BPS08(GS)]	(BPS08)	$8.46^{+0.87}_{-0.88}$	$127.9^{+8.1}_{-8.2}$

[tb] Results from real time solar-neutrino experiments. The predictions of the standard solar model BPS08(GS) are also shown. The first and the second errors in the experimental results are the statistical and systematic errors, respectively.

Ref.		Reaction	^{8}B ν flux $(10^6\ \mathrm{cm}^{-2}\mathrm{s}^{-1})$	^{7}Be ν flux $(10^9\ \mathrm{cm}^{-2}\mathrm{s}^{-1})$
Kamiokande (Fukuda96)	ν_e	$2.80 \pm 0.19 \pm 0.33$	—	
Super-Kamiokande (Hosaka06)	ν_e	$2.35 \pm 0.02 \pm 0.08$	—	
SNO Phase I (Ahmad02)	CC	$1.76^{+0.06}_{-0.05} \pm 0.09$	—	
(pure D_2O)		ν_e	$2.39^{+0.24}_{-0.23} \pm 0.12$	—
		NC	$5.09^{+0.44+0.46}_{-0.43-0.43}$	—
SNO Phase II (Aharmim05)	CC	$1.68 \pm 0.06^{+0.08}_{-0.09}$	—	
(NaCl in D_2O)		ν_e	$2.35 \pm 0.22 \pm 0.15$	—
		NC	$4.94 \pm 0.21^{+0.38}_{-0.34}$	—
SNO Phase III (Aharmim08)	CC	$1.67^{+0.05+0.07}_{-0.04-0.08}$	—	
(^{3}He counters)		ν_e	$1.77^{+0.24+0.09}_{-0.21-0.10}$	—
		NC	$5.54^{+0.33+0.36}_{-0.31-0.34}$	—
SNO Phase I+II (Aharmim09)	NC	$5.140^{+0.160+0.132}_{-0.158-0.117}$	—	
(Joint Analysis)		fit to all data	$5.046^{+0.159+0.107}_{-0.152-0.123}$	—
Borexino (Arpesella08b)		ν_e	—	3.36 ± 0.34
SSM [BPS08(GS)]			$5.94(1 \pm 0.11)$	$5.07(1 \pm 0.06$

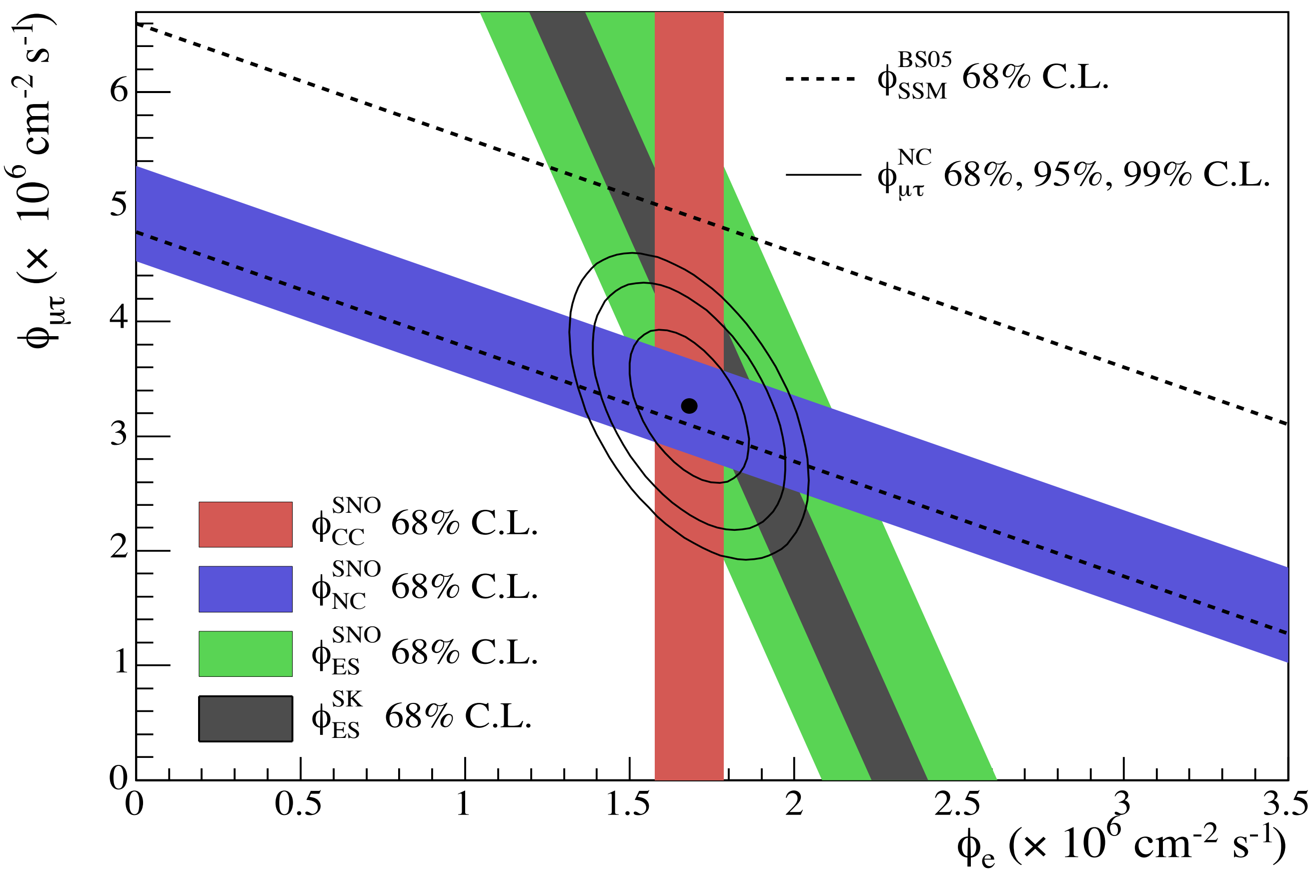
ϕ_{SSM}^{BS05} 68% C.L.
$\phi_{\mu\tau}^{NC}$ 68%, 95%, 99% C.L.
ϕ_{CC}^{SNO} 68% C.L.
ϕ_{NC}^{SNO} 68% C.L.
ϕ_{ES}^{SNO} 68% C.L.
ϕ_{ES}^{SK} 68% C.L.
$\phi_{\mu\tau}$ ($\times$ 10^6 cm^{-2} s^{-1})
ϕ_e ($\times$ 10^6 cm^{-2} s^{-1})
0
1
2
3
4
5
6
0
0.5
1
1.5
2
2.5
3
3.5

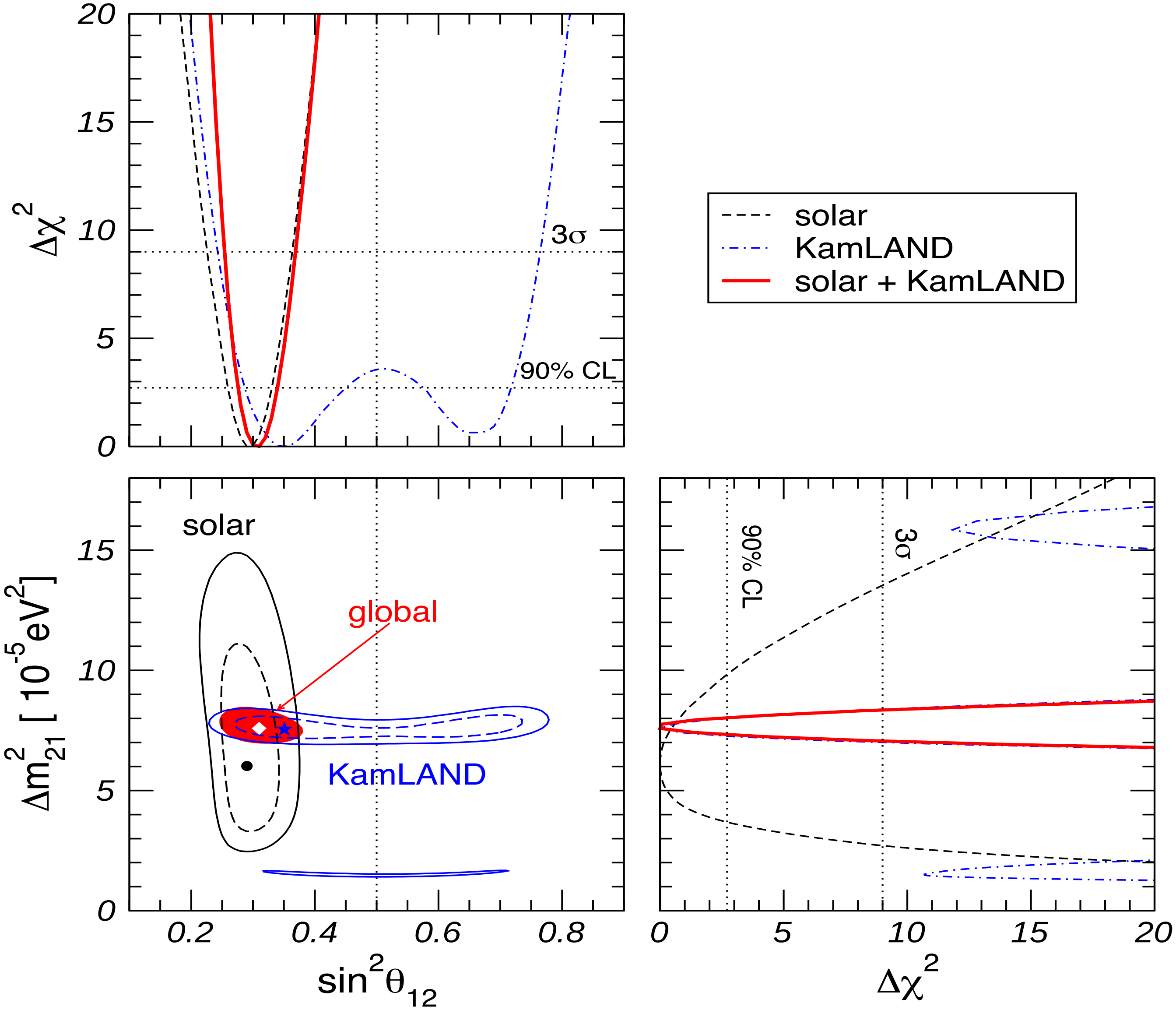

T. Schwetz, M.Tortola, J.F.W. Valle, 2008/2010

$3-\nu$ Mixing Analysis: $\Delta m^2_{\odot} \ll |\Delta m^2_{\rm atm}|$

$$P^{3\nu}_{\odot} \cong \sin^4\theta_{13} + \cos^4\theta_{13}\ P^{2\nu}_{\odot},$$

$$P^{2\nu}_{\odot} = \bar{P}^{2\nu}_{\odot} + P^{2\nu}_{\odot\ \rm osc},$$

$$\bar{P}^{2\nu}_{\odot} = \frac{1}{2} + (\frac{1}{2} - P')\cos 2\theta^m_{12}(t_0)\cos 2\theta_{12} \qquad (\theta_{12} \equiv \theta_{\odot}),$$

$P' = 0$: L. Wolfenstein, 1978; S. Mikheyev, A. Smirnov, 1985;

$P' \neq 0$ (general or LZ): S. Parke, W. Haxton, 1986;

P' exp. decreasing N_e, $P^{2\nu}_{\odot\ \rm osc}$: S.T.P., 1988

$$N_e \rightarrow N_e \cos^2\theta_{13},$$

$$P' = \frac{e^{-2\pi r_0 \frac{\Delta m^2}{2E}\sin^2\theta_{12}} - e^{-2\pi r_0 \frac{\Delta m^2}{2E}}}{1 - e^{-2\pi r_0 \frac{\Delta m^2}{2E}}}, \qquad r_0 \sim 0.1 R_{\odot}$$

S.T.P., 1988

LMA: $P' \ll 1, \quad < P^{2\nu}_{\odot\ \rm osc} > \cong 0$

J. Rich, S.T.P., 1988

$$P^{3\nu}_{\rm KL} \cong \sin^4\theta_{13} + \cos^4\theta_{13}\left[1 - \sin^2 2\theta_{12}\sin^2(\frac{\Delta m^2_{\odot}}{4E}L)\right]$$

$$P^{3\nu}_{\rm CHOOZ} \cong 1 - \sin^2 2\theta_{13}\sin^2(\frac{\Delta m^2_{\rm atm}}{4E}L)$$

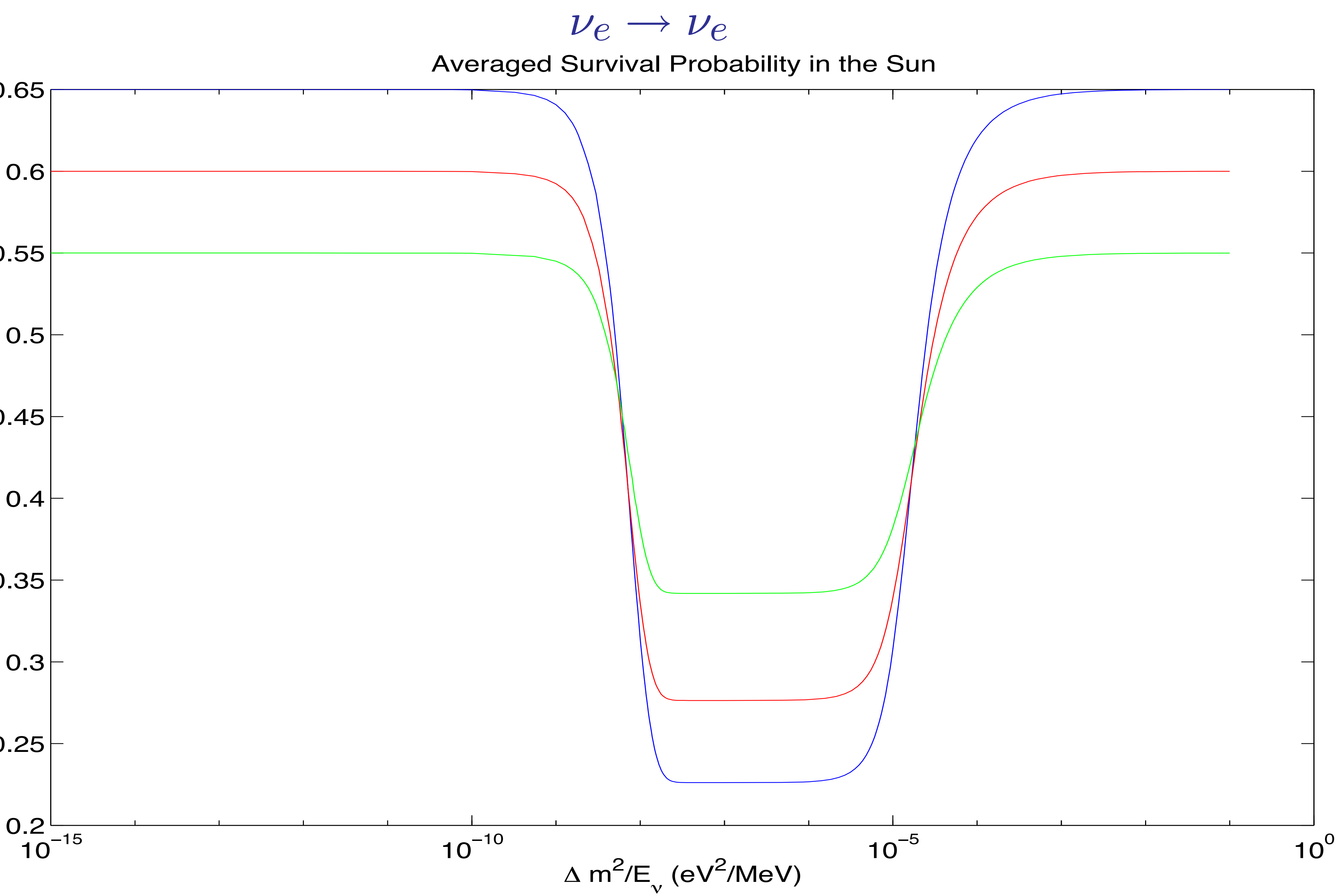

$\nu_e \longrightarrow \nu_e$
Averaged Survival Probability in the Sun
0.65
0.6
0.55
0.5
0.45
0.4
0.35
0.3
0.25
0.2
10^{-15}
10^{-10}
10^{-5}
10^{0}
$\Delta m^2/E_\nu$ (eV^2/MeV)

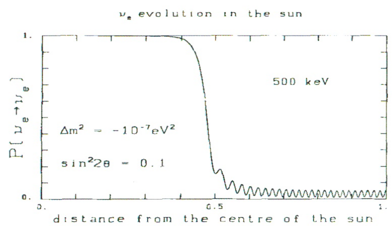

Fig. 4. ν_e oscillations in the solar matter. The probability $P(\nu_e \to \nu_e)$ is plotted as a function of the distance to the solar centre where the neutrinos are produced (no spatial distribution is assumed in this figure). The figure corresponds to a 500 keV neutrino for $\Delta m^2 = -10^{-7}\,\mathrm{eV}^2$ and $\sin^2 2\theta = 0.1$

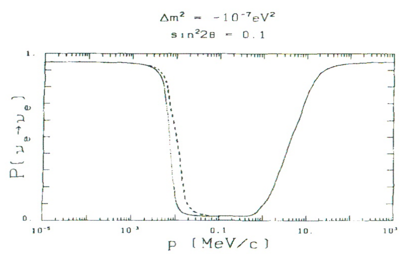

Fig. 5. Probability $P(\nu_e \to \nu_e)$ as a function of the neutrino momentum p in MeV/c for $\sin^2 2\theta = 0.1$ and $\Delta m^2 = -10^{-7}\,\mathrm{eV}^2$. The full curve corresponds to neutrinos produced at the centre of the sun and going until the surface. The dashed curve corresponds to neutrinos produced according to the radial distribution predicted by the SSM. The results are averaged over one oscillation length

and the value at the surface which depend on θ would be different.

Figure 5 shows P at the surface of the sun (averaged over one vacuum oscillation length) as a function of neutrino energy. As above the calculation is done for $\Delta m^2 = -10^{-7}\,\mathrm{eV}^2$ and $\sin^2 2\theta = 0.1$. The full curve corresponds to neutrinos produced at the center of the sun. The dashed curve is obtained by averaging neutrinos produced according to a radial distribution similar to that predicted by the SSM [19]. Equations (18) give $p_{\min} = 7.5$ keV/c and $p_{\max} = 2$ MeV/c and the flux is seen to be suppressed between these limits for neutrinos produced at the center. For neutrinos produced according to the real radial distribution, the effective $p_{\min}$ is higher, as expected. The minimum value between $p_{\min}$ and $p_{\max}$ is equal to $\sin^2\theta$.

Most of the results below correspond to $P(\nu_e \to \nu_e)$ as a function of Δm^2. Each point corresponds to the mean

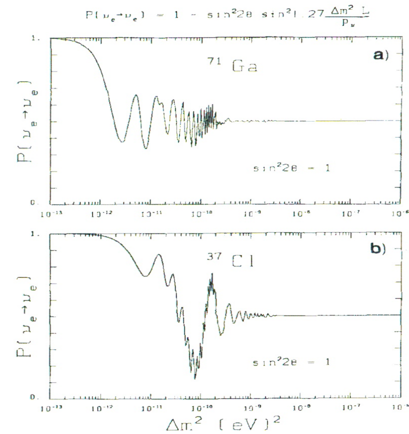

Fig. 6a, b. Probability $P(\nu_e \to \nu_e)$ as a function of Δm^2 for solar ν_e in vacuum observed at the earth. The figure corresponds to the maximum mixing angle $\sin^2 2\theta = 1$. **a** gallium experiment. **b** chlorine experiment

value of about 500 neutrinos generated with the solar spectrum described above. We will present successively the results in vacuum, the results in solar matter with $\Delta m^2 < 0$ and with $\Delta m^2 > 0$. The earth effects have been taken into account.

Figure 6 presents the results obtained in vacuum (i.e. without any effect due to matter) for solar neutrinos travelling from the sun to the earth. The results are obtained for chlorine and gallium detectors and correspond to a maximum mixing angle. They are very similar to the ones previously shown by Hampel [3].

Figure 7 presents the results obtained by taking into account the solar matter and the earth matter averaged over the day and the year. They are given for the gallium detector for different values of $\sin^2 2\theta$ for $\Delta m^2 < 0$ (i.e. $m_1^2 < m_2^2$). It is very clear on this figure that the effect of matter is to reduce by a considerable factor the probability of observing ν_e if Δm^2 falls in some range which depends on $\sin^2 2\theta$. This range can be determined qualitatively from (14) and (15) by taking a neutrino energy of 500 keV which is near the average detected neutrino energy for the gallium experiment according to the SSM. The effect of the solar matter has two characteristics: the Δm^2 range affected decreases when $\sin^2 2\theta$ decreases as shown by (15) but the intensity of the effect remains important when $\sin^2\theta$ decreases up to values as small as 0.001.

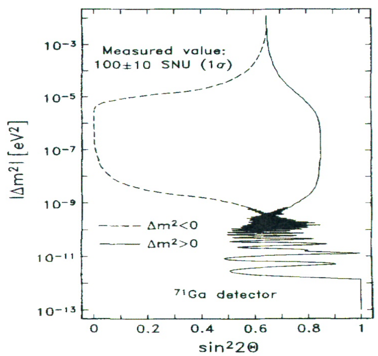

Fig. 12. Example of a $\Delta m^2 - \sin^2 2\theta$ exclusion plot to be obtained with the gallium detector. The area to the right of the curves is excluded with 90% C.L. if the measured signal is 100 ± 10 SNU. The solid line is for $\Delta m^2 > 0$ and the dashed line for $\Delta m^2 < 0$. Below 10^{-9} eV^2 the solid line is valid for both cases

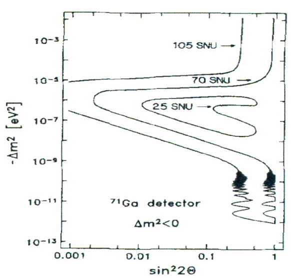

Fig. 13. $\Delta m^2 - \sin^2 2\theta$ plot for the gallium experiment. The curves indicate the allowed values for Δm^2 and $\sin^2 2\theta$ if the measured rate is 105, 70 or 25 SNU

9. Conclusion

We analyzed in this paper the effects of the solar and earth matter on the solar neutrino flux. We confirm that a large suppression (> 30%) of the solar neutrino flux may be obtained for some values of $m_2^2 - m_1^2$

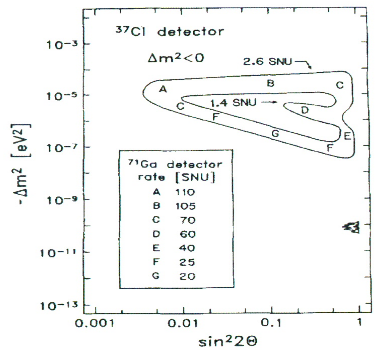

Fig. 14. $\Delta m^2 - \sin^2 2\theta$ plot for the chlorine experiment. The band represents the 2σ range of the experimental result (1.4 – 2.6 SNU). The letters within the band indicate the possible signals (in SNU) to be obtained with the gallium detector

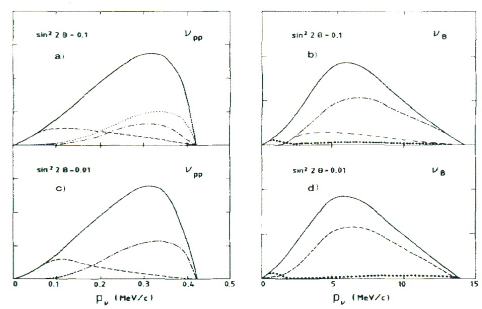

Fig. 15a–d. Spectrum of neutrinos produced by the pp fusion reaction **a**, **c** or by the ^{8}B decay reaction **b**, **d**. The different dotted or dashed lines are the expected spectrum shapes at the earth when assuming oscillations in the solar and earth matter with different values of $\sin^2 2\theta$ and Δm^2. The full curves correspond to the theoretical spectrum or to the spectrum without matter effect. The dotted curve is for $\Delta m^2 = -10^{-8}$ eV^2. The dashed-dotted curve is for $\Delta m^2 = -10^{-7}$ eV^2. The dashed curve is for $\Delta m^2 = -10^{-6}$ eV^2. The curve with full circles is for $\Delta m^2 = -10^{-5}$ eV^2

around $10^{-4} - 10^{-8}$ eV^2 even for small mixing angles ($\sin^2 2\theta = 10^{-1}$ to 10^{-3}). The earth effects are small compared to the sun effects but cannot be neglected. All this increases the interest in the expected result of the forthcoming gallium experiment since the observed

MSW Transitions of Solar Neutrinos in the Sun (and the Hydrogen Atom)

$$i\frac{d}{dt}\begin{pmatrix} A_\alpha(t,t_0) \\ A_\beta(t,t_0) \end{pmatrix} = \begin{pmatrix} -\epsilon(t) & \epsilon'(t) \\ \epsilon'(t) & \epsilon(t) \end{pmatrix} \begin{pmatrix} A_\alpha(t,t_0) \\ A_\beta(t,t_0) \end{pmatrix} \qquad (1)$$

where $\alpha = \nu_e$, $\beta = \nu_{\mu(\tau)}$,

$\epsilon(t) = \frac{1}{2}\,[\frac{\Delta m^2}{2E}\cos 2\theta - \sqrt{2}G_F N_e(t)]$,

$\epsilon'(t) = \frac{\Delta m^2}{4E}\sin 2\theta$, with $\Delta m^2 = m_2^2 - m_1^2$.

- Standard Solar Models

$N_e(t) = N_e(t_0)\exp\left\{-\frac{t-t_0}{r_0}\right\}$, $r_0 \sim 0.1 R_\odot$, $R_\odot = 6.96 \times 10^5$km

Introducing the dimensionless variable

$$Z = ir_0\sqrt{2}G_F N_e(t_0)e^{-\frac{t-t_0}{r_0}}, \quad Z_0 = Z(t = t_0),$$

and making the substitution

$$A_e(t,t_0) = (Z/Z_0)^{c-a}\ e^{-(Z-Z_0)+i\int_{t_0}^{t}\epsilon(t')dt'}\ A'_e(t,t_0),$$

$A'_e(t,t_0)$ satisfies the confluent hypergeometric equation (CHE):

$$\left\{\ Z\frac{d^2}{dZ^2} + (c - Z)\ \frac{d}{dZ} - a\right\} A'_e(t,t_0) = 0,$$

where

$$a = 1 + ir_0\ \frac{\Delta m^2}{2E}\sin^2\theta, \qquad c = 1 + ir_0\ \frac{\Delta m^2}{2E}.$$

The confluent hypergeometric equation describing the ν_e oscillations in the Sun, coincides in form with the Schroedinger (energy eigenvalue) equation obeyed by the radial part, $\psi_{kl}(r)$, of the non-relativistic wave function of the hydrogen atom,

$\Psi(\overrightarrow{r}) = \frac{1}{r}\psi_{kl}(r)Y_{lm}(\theta', \phi')$,

r, θ' and ϕ' are the spherical coordinates of the electron in the proton's rest frame, l and m are the orbital momentum quantum numbers ($m = -l, ..., l$), k is the quantum number labeling (together with l) the electron energy (the principal quantum number is equal to $(k+l)$), E_{kl} ($E_{kl} < 0$), and $Y_{lm}(\theta', \phi')$ are the spherical harmonics. The function

$\psi'_{kl}(Z) = Z^{-c/2}\ e^{Z/2}\ \psi_{kl}(r)$

satisfies the confluent hypergeometric equation in which the variable Z and the parameters a and c are in this case related to the physical quantities characterizing the hydrogen atom:

$$Z = 2\ \frac{r}{a_0}\sqrt{-E_{kl}/E_I},\ \ a \equiv a_{kl} = l + 1 - \sqrt{-E_I/E_{kl}},\ \ c \equiv c_l = 2(l+1),$$

$a_0 = \hbar/(m_e e^2)$ is the Bohr radius and $E_I = m_e e^4/(2\hbar^2) \cong 13.6\ eV$ is the ionization energy of the hydrogen atom.

Any solution - linear combination of two linearly independent solutions:

$\Phi(a,c;Z)$, $Z^{1-c}\ \Phi(a-c+1,2-c;Z)$; $\Phi(a',c';Z=0)=1$, $a',c'\neq 0,-1,-2,....$

$$A(\nu_e \rightarrow \nu_{\mu(\tau)}) = \frac{1}{2}\ \sin 2\theta\ \left\{\Phi(a-c,2-c;Z_0) - e^{i(t-t_0)\frac{\Delta m^2}{2E}}\ \Phi(a-1,c;Z_0)\ \right\}.$$

Sun: $N_e(x) \cong N_e(x_0) e^{-\frac{x}{r_0}}$, $r_0 \cong 0.1 R_\odot$, $R_\odot \cong 7\times 10^5$ km

The region of $\nu_\odot$ production:

20 $N_A\ cm^{-3} \lesssim N_e(x_0) \lesssim 100\ N_A\ cm^{-3}$: $|Z_0| > 500$ (!)

The solar ν_e survival probability:

$$\bar{P}(\nu_e \rightarrow \nu_e) = \tfrac{1}{2} + (\tfrac{1}{2} - P')\cos 2\theta_m^0 \cos 2\theta,$$

$$P' = \frac{e^{-2\pi r_0 \frac{\Delta m^2}{2E}\sin^2\theta} - e^{-2\pi r_0 \frac{\Delta m^2}{2E}}}{1 - e^{-2\pi r_0 \frac{\Delta m^2}{2E}}}$$

S.T.P., 1988

The solar ν_e survival probability:

$$\bar{P}(\nu_e \to \nu_e) = \frac{1}{2} + (\frac{1}{2} - P') \cos 2\theta_m^0 \cos 2\theta,$$

$$P' = \frac{e^{-2\pi r_0 \frac{\Delta m^2}{2E} \sin^2\theta} - e^{-2\pi r_0 \frac{\Delta m^2}{2E}}}{1 - e^{-2\pi r_0 \frac{\Delta m^2}{2E}}}, \quad \Delta m^2 > 0$$

Case 1: $\cos 2\theta_m^0 = -1,\ P' = 0,\ \bar{P} = \frac{1}{2}(1 - \cos 2\theta)$.

Case 2: $\theta_m^0 = \theta,\ P' = 0,\ \bar{P}(\nu_e \to \nu_e) = 1 - \frac{1}{2}\sin^2 2\theta$

Case 1: SNO, Super Kamiokande; $\bar{P} \cong 0.3$: $\cos 2\theta > 0$!

Case 2: pp neutrinos.

The solar ν_e transitions observed by SK, SNO:

$$\text{MSW}: \quad P_{\odot}^{3\nu} \cong \sin^4\theta_{13} + \cos^4\theta_{13}\ \sin^2\theta_{12}\,.$$

In the case of oscillations in vacuum:

$$P_{\odot}^{3\nu} \cong \sin^4\theta_{13} + (1 - 0.5\sin^2 2\theta_{12})\cos^4\theta_{13} \gtrsim 0.48$$

$$(\sin^2\theta_{13} < 0.053,\ \ \sin^2 2\theta_{12} \lesssim 0.93)\,.$$

Data: $P_{\odot}^{3\nu} \cong 0.3$ - a strong evidence for matter effects in the solar ν_e transitions.

G.L. Fogli *et al.*, 2004

Atmospheric Neutrinos

Zenith angle distributions

$\nu_\mu \leftrightarrow \nu_\tau$
2-flavor oscillations

Best fit
$\sin^2 2\theta=1.0$, $\Delta m^2=2.0\times10^{-3}$ eV^2
Null oscillation

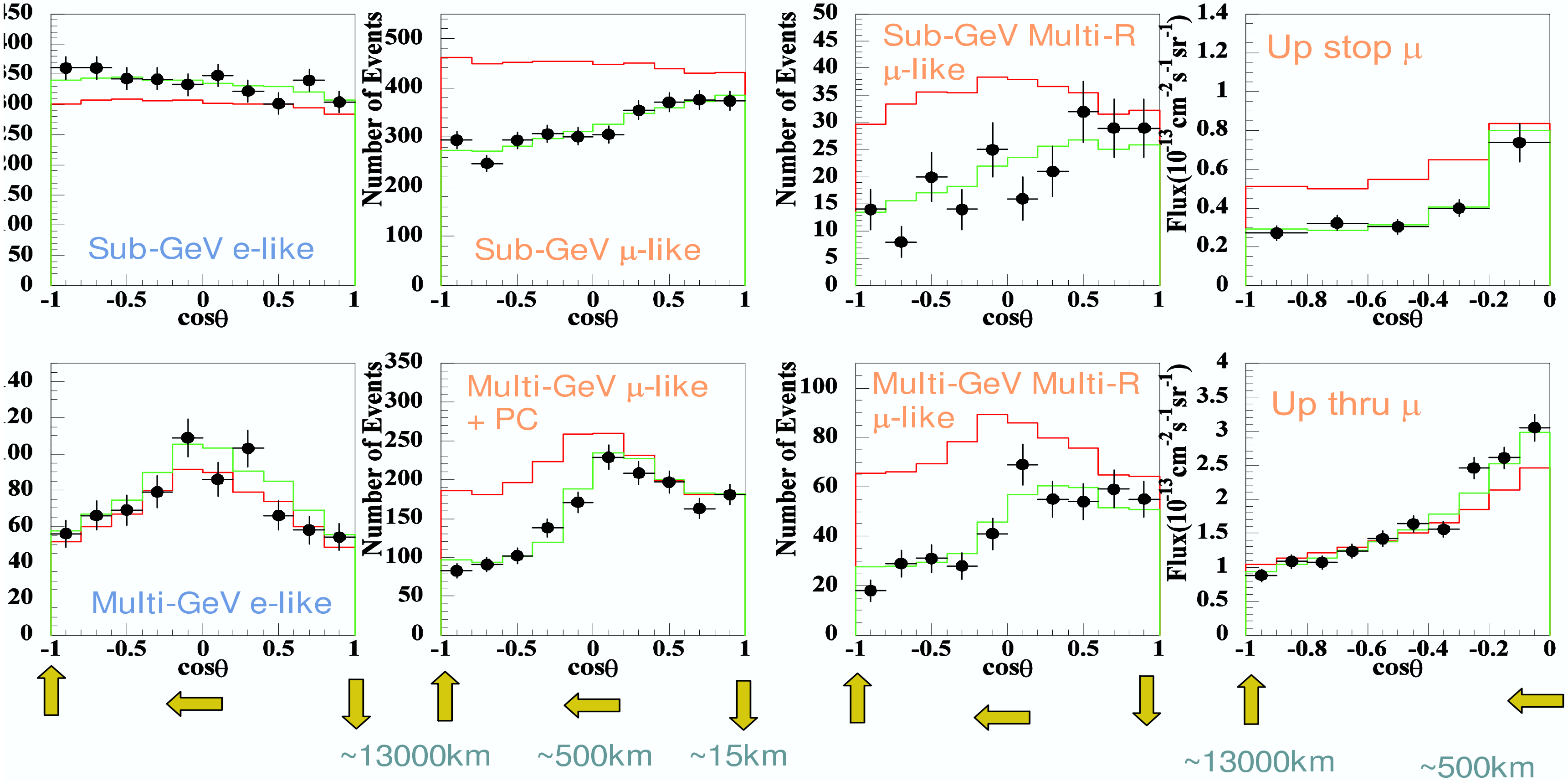

Observing the Oscillations of Neutrinos

SK: L/E Dependence, μ–Like Events

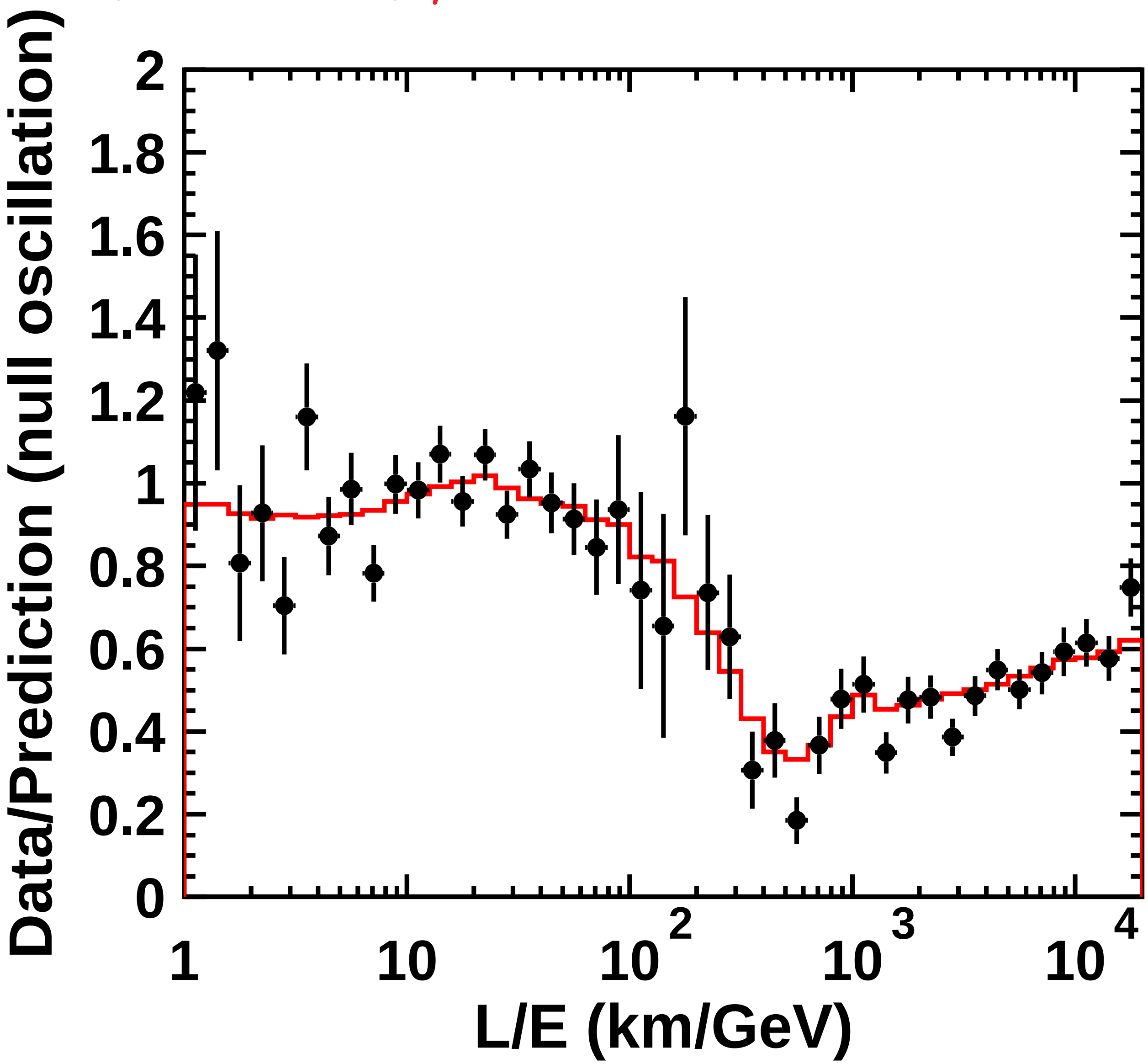

L/E dependence of $P_{\rm osc}$: V. Gribov, B. Pontecorvo, 1969

L/E analysis

Neutrino oscillation : $P_{\mu\mu} = 1 - \sin^2 2\theta \sin^2(1.27 \frac{\Delta m^2 L}{E})$

Neutrino decay : $P_{\mu\mu} = (\cos^2\theta + \sin^2\theta \times \exp(-\frac{m}{2\tau}\frac{L}{E}))^2$

Neutrino decoherence : $P_{\mu\mu} = 1 - \frac{1}{2}\sin^2 2\theta \times (1 - \exp(-\gamma_0 \frac{L}{E}))$

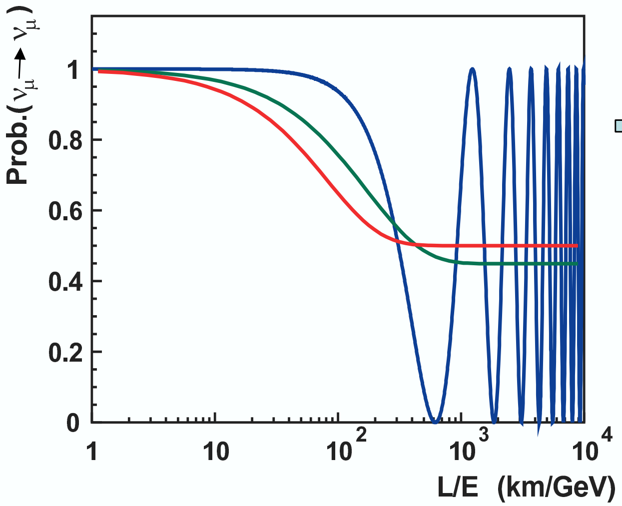

Use events with high resolution in L/E

The first dip can be observed

→ Direct evidence for oscillations

→ Strong constraint to oscillation parameters, especially Δm^2 value

K2K: ν_μ Spectrum

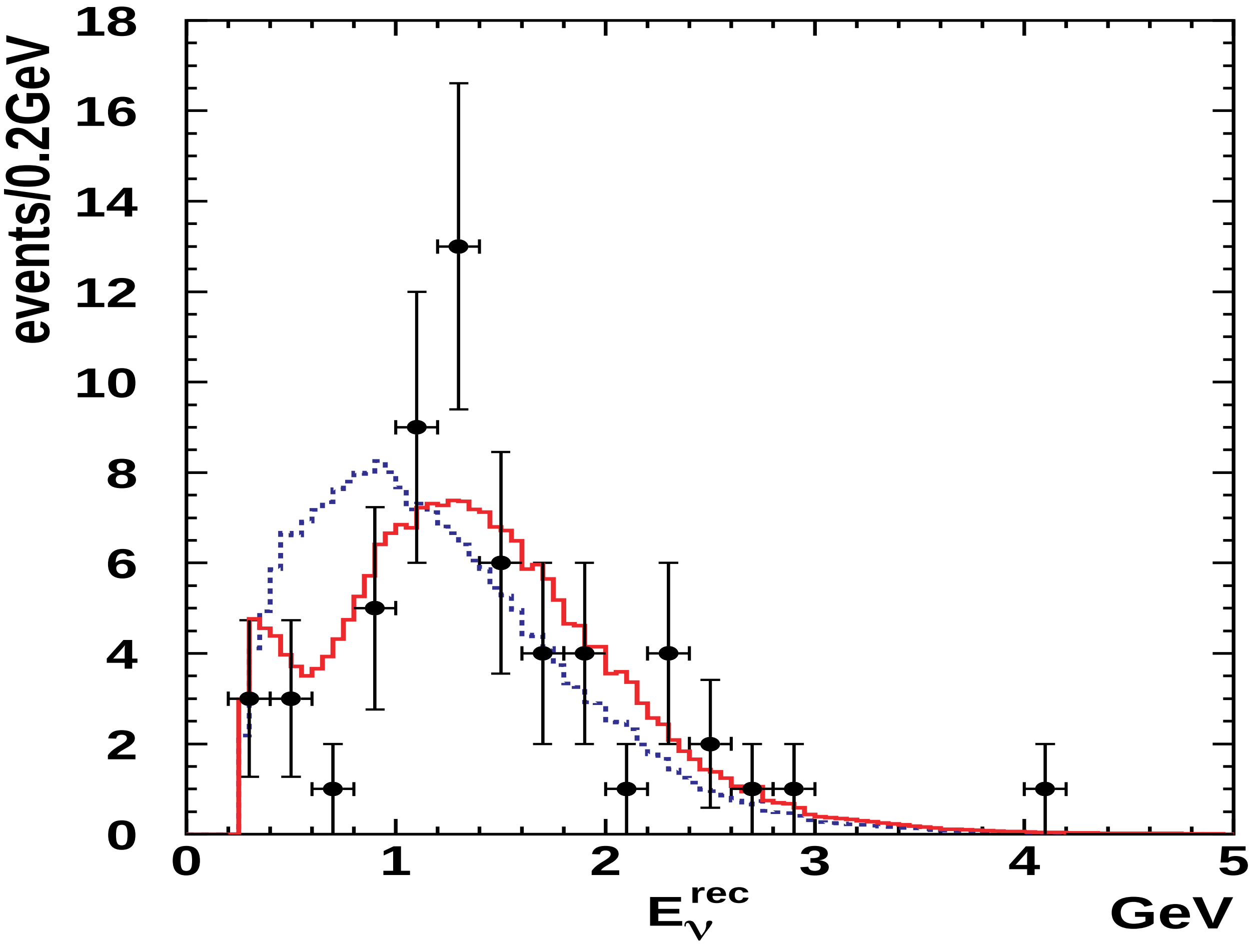

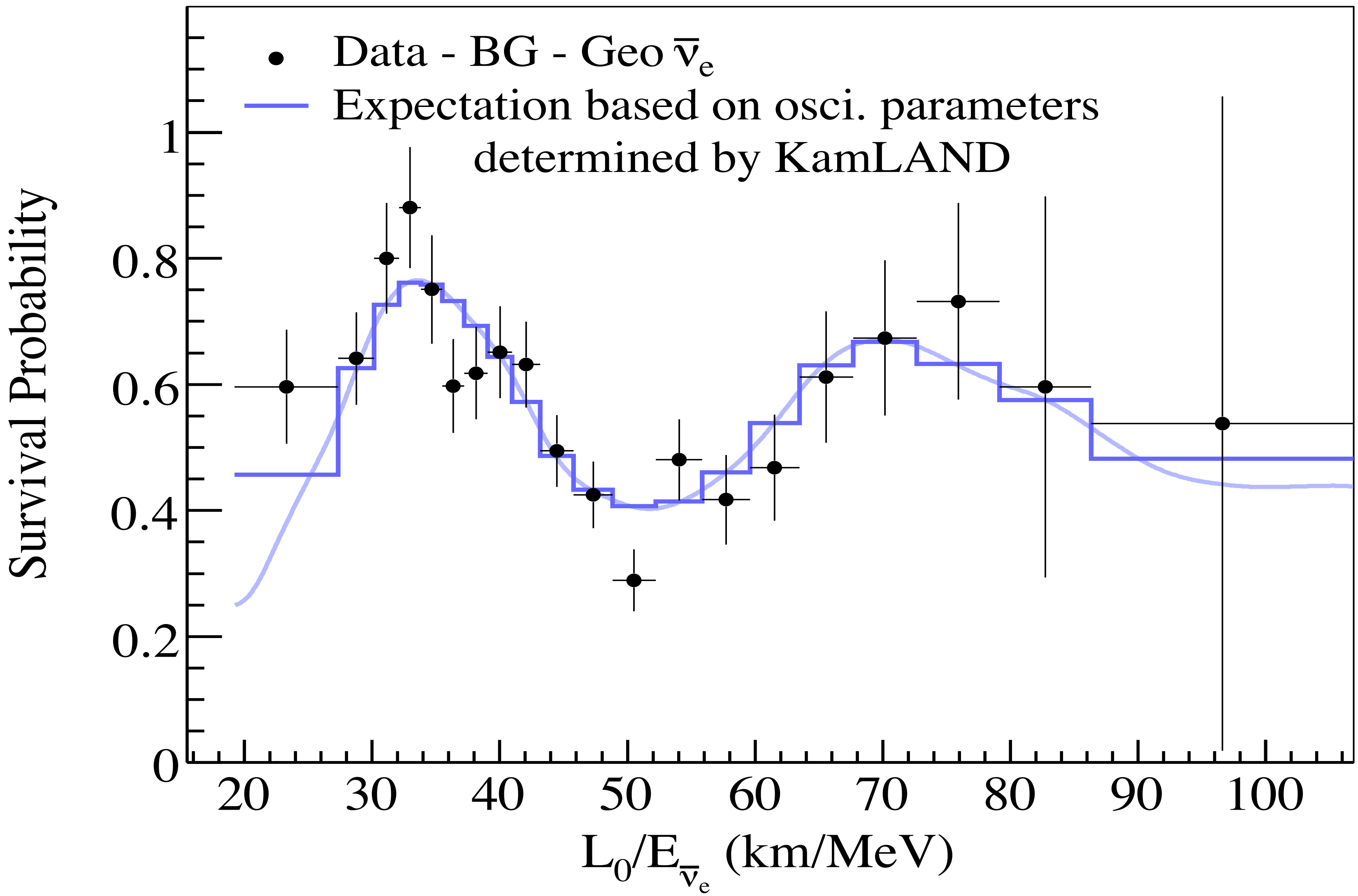

KamLAND: $L/E-$Dependence

$\bar{\nu}_e \longrightarrow \bar{\nu}_e$

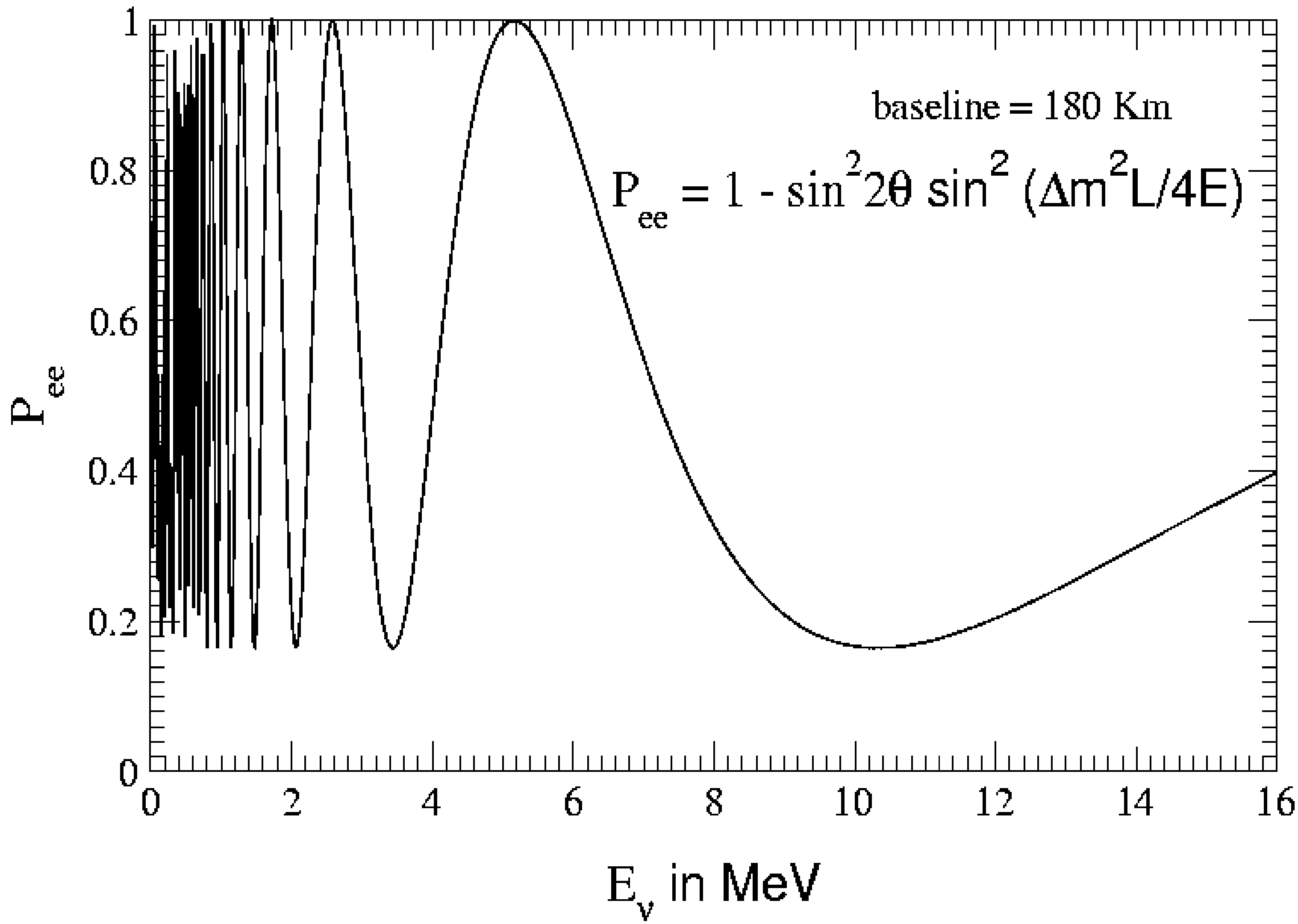

MINOS: ν_μ Spectrum

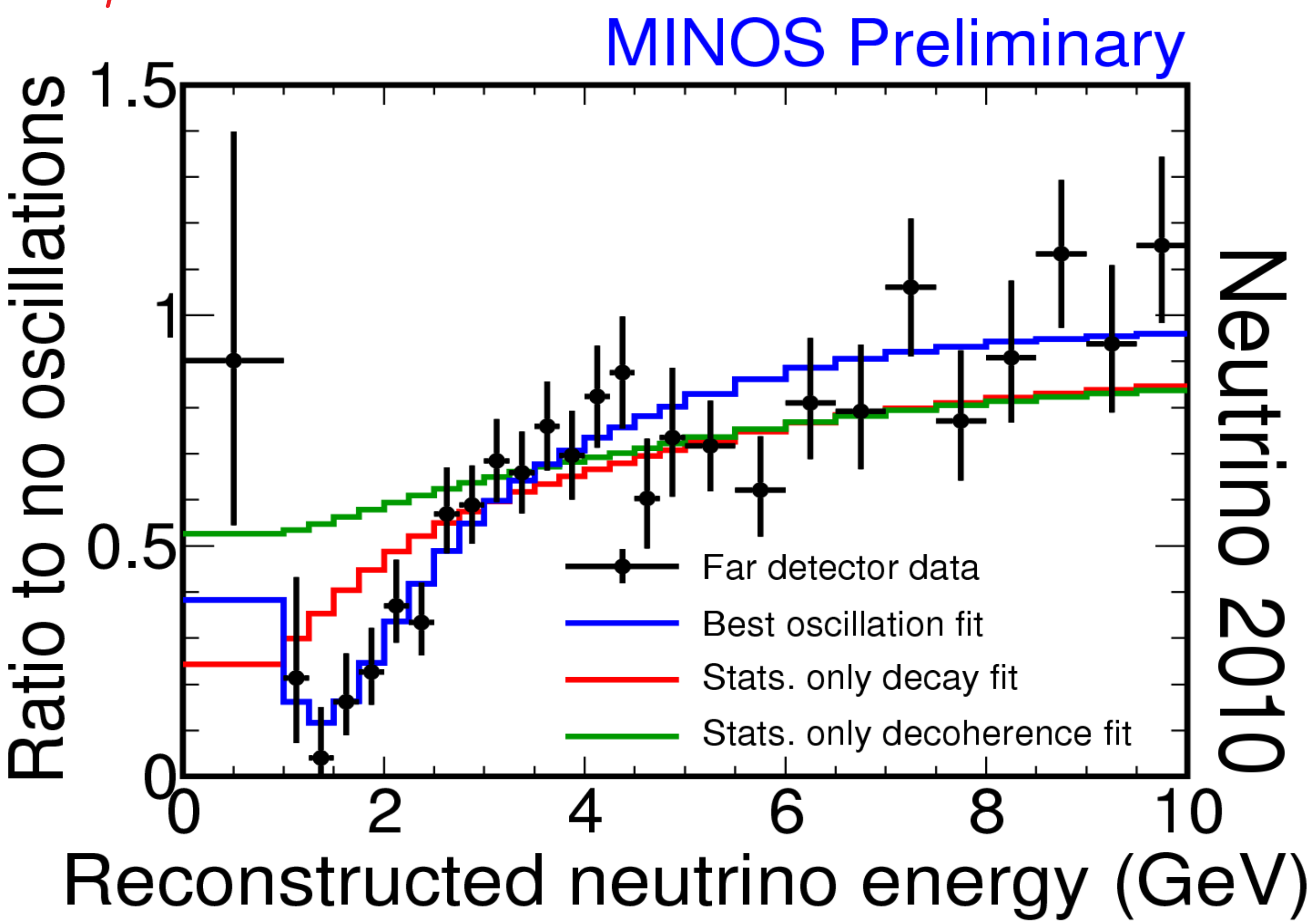

Compelling Evidences for $\nu-$Oscillations: 3-ν mixing

$$\nu_{l\mathrm{L}} = \sum_{j=1} U_{lj}\, \nu_{j\mathrm{L}} \qquad l = e, \mu, \tau.$$

QM of Neutrino Oscillations in Vacuum

$$A(\nu_l \to \nu_{l'}) = \sum_j U_{l'j}\, D_j\, U^{\dagger}_{jl}\,, \quad l, l' = e, \mu, \tau\,,$$

$$D_j = e^{-i\tilde{p}_j\,(x_f - x_0)} = e^{-i(E_jT - p_jL)}\,, \qquad p_j \equiv |\mathbf{p}_j|\,.$$

$$\delta\varphi_{jk} = (E_j - E_K)T - (p_j - p_k)L$$
$$= (E_j - E_K)\left[T - \frac{E_j+E_K}{p_j+p_k}\,L\right] + \frac{m_j^2-m_k^2}{p_j+p_k}\,L\,;$$

First term - negligible:

- L and T related: $T = (E_j + E_k)\,L/(p_j + p_k) = L/\bar{v}$,

$\bar{v} = (E_j/(E_j + E_k))v_j + (E_k/(E_j + E_k))v_k$ - the "average" velocity of ν_j and ν_k, $v_{j,k} = p_{j,k}/E_{j,k}$;

- $E_j = E_k = E_0$;
- $p_j = p_k = p$

(additionally suppressed by $(m_j^2 + m_k^2)/p^2$: $L = T$ up to $\sim m_{j,k}^2/p^2$);

- $E_j \neq E_k$, $p_j \neq p_k$, $j \neq k$: the same conclusion

(neutrinos are relativistic, $L \cong T$ up to corrections $\sim m_{j,k}^2/E_{j,k}^2$).

$$\delta\varphi_{jk} \cong \frac{m_j^2 - m_k^2}{2p} L = 2\pi \frac{L}{L_{jk}^v} \operatorname{sgn}(m_j^2 - m_k^2)\,, \quad p = (p_j + p_k)/2,$$

$$L_{jk}^v = 4\pi \frac{p}{|\Delta m_{jk}^2|} \cong 2.5 \text{ m } \frac{p[MeV]}{|\Delta m_{jk}^2|[eV^2]}$$

is the neutrino oscillation length associated with Δm_{jk}^2.

- One can safely neglect the dependence of p_j and p_k on the masses m_j and m_k and consider p to be the zero neutrino mass momentum, $p = E$.
- The phase $\delta\varphi_{jk}$ is Lorentz invariant.

$$\sigma_{m^2} = \sqrt{(2E\sigma_E)^2 + (2p\sigma_p)^2}$$

Condition for producing coherently $\nu_1, \nu_2, ...$:

$$\sigma_{m^2} > \Delta m_{jk}^2$$

The equation used above corresponds to a plane wave description of the propagation of neutrinos ν_j. It accounts only for the movement of the center of the wave packet describing ν_j. In the wave packet treatment of the problem, the interference between the states of ν_j and ν_k is subject to a number of conditions, the localisation condition (in space and time) and the condition of overlapping of the wave packets of ν_j and ν_k at the detection point being the most important. For relativistic neutrinos, the localisation condition in space reads: $\sigma_{xP}, \sigma_{xD} < L^v_{jk}/(2\pi)$, $\sigma_{xP(D)}$ being the spatial width of the production (detection) wave packet. Thus, the interference will not be suppressed if the spatial width of the neutrino wave packets detetermined by the neutrino production and detection processes is smaller than the corresponding oscillation length in vacuum. In order for the interference to be nonzero, the wave packets describing ν_j and ν_k should also overlap in the point of neutrino detection. This requires that the spatial separation between the two wave packets at the point of neutrinos detection, caused by the two wave packets having different group velocities $v_j \neq v_k$, satisfies $|(v_j - v_k)T| \ll \max(\sigma_{xP}, \sigma_{xD})$. If the interval of time T is not measured, T in the preceding condition must be replaced by the distance L between the neutrino source and the detector.

Examples

- Spatial localisation condition

ΔL - dimensions of the ν- source (and/or detector):

$2\pi \Delta L / L^{v}_{jk} \lesssim 1.$

- Time localisation condition

ΔE - detector's energy resolution:

$2\pi (L/L^{v}_{jk})(\Delta E/E) \lesssim 1.$

If $2\pi \Delta L / L^{v}_{jk} \gg 1$, and/or $2\pi (L/L^{v}_{jk})(\Delta E/E) \gg 1$,

$\bar{P}(\nu_l \to \nu_{l'}) = \bar{P}(\bar{\nu}_l \to \bar{\nu}_{l'}) \cong \sum_j |U_{l'j}|^2 \, |U_{lj}|^2$

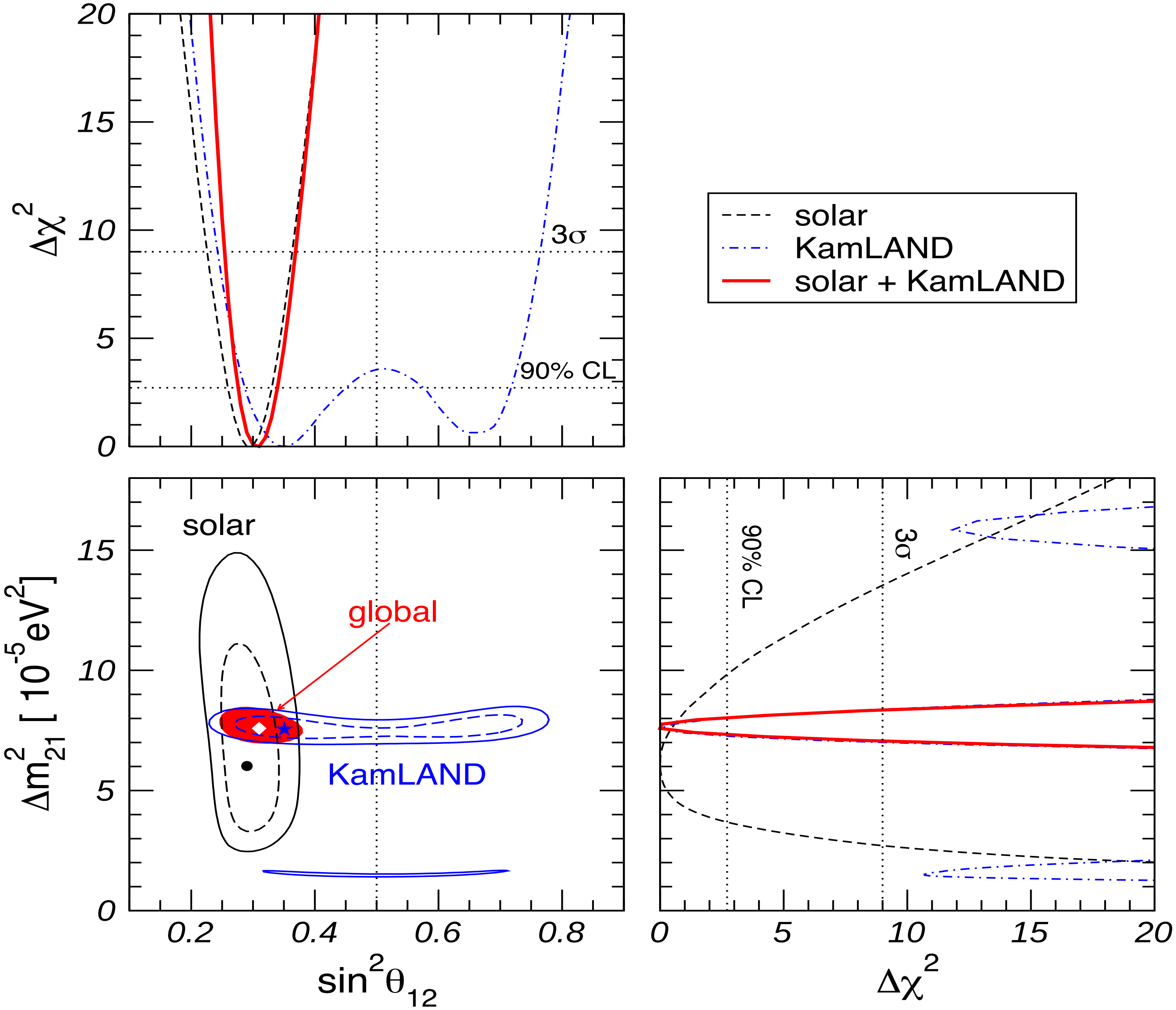

T. Schwetz, M.Tortola, J.F.W. Valle, 2008/2010

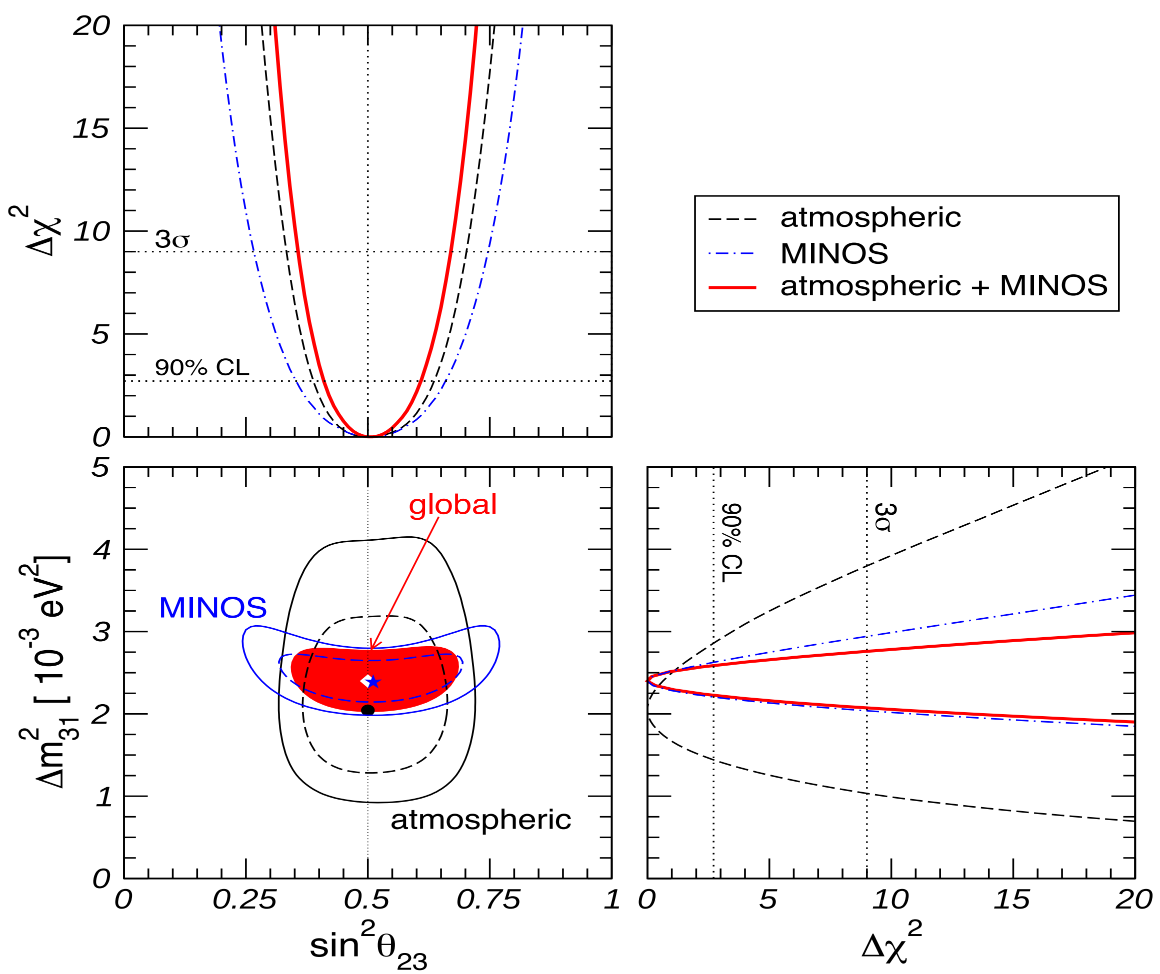

T. Schwetz, M.Tortola, J.F.W. Valle, 2008/2010

- sign of $\Delta m^2_{\rm atm}$ not determined;

3-ν mixing: $\Delta m^2_{31} > 0$, $m_1 < m_2 < m_3$ (normal ordering (NO));

$\Delta m^2_{31} < 0$, $m_3 < m_1 < m_2$ (inverted ordering (IO)).

- If $\theta_{23} \neq \frac{\pi}{4}$: θ_{23}, $(\frac{\pi}{4} - \theta_{23})$ ambiguity.

Three Neutrino Mixing

$$\nu_{l\mathrm{L}} = \sum_{j=1}^{3} U_{lj}\, \nu_{j\mathrm{L}} \ .$$

U is the Pontecorvo-Maki-Nakagawa-Sakata (PMNS) neutrino mixing matrix,

$$U = \begin{pmatrix} U_{e1} & U_{e2} & U_{e3} \\ U_{\mu 1} & U_{\mu 2} & U_{\mu 3} \\ U_{\tau 1} & U_{\tau 2} & U_{\tau 3} \end{pmatrix}$$

- U - $n \times n$ unitary:

	n	2	3	4
mixing angles:	$\frac{1}{2}n(n-1)$	1	3	6
CP-violating phases:				
• ν_j- Dirac:	$\frac{1}{2}(n-1)(n-2)$	0	1	3
• ν_j- Majorana:	$\frac{1}{2}n(n-1)$	1	3	6

$n = 3$: 1 Dirac and
2 additional CP-violating phases, Majorana phases

S.M. Bilenky, J. Hosek, S.T.P., 1980

PMNS Matrix: Standard Parametrization

$$U = V \begin{pmatrix} 1 & 0 & 0 \\ 0 & e^{i\frac{\alpha_{21}}{2}} & 0 \\ 0 & 0 & e^{i\frac{\alpha_{31}}{2}} \end{pmatrix}$$

$$V = \begin{pmatrix} c_{12}c_{13} & s_{12}c_{13} & s_{13}e^{-i\delta} \\ -s_{12}c_{23} - c_{12}s_{23}s_{13}e^{i\delta} & c_{12}c_{23} - s_{12}s_{23}s_{13}e^{i\delta} & s_{23}c_{13} \\ s_{12}s_{23} - c_{12}c_{23}s_{13}e^{i\delta} & -c_{12}s_{23} - s_{12}c_{23}s_{13}e^{i\delta} & c_{23}c_{13} \end{pmatrix}$$

- $s_{ij} \equiv \sin\theta_{ij}$, $c_{ij} \equiv \cos\theta_{ij}$, $\theta_{ij} = [0, \frac{\pi}{2}]$,
- δ - Dirac CP-violation phase, $\delta = [0, 2\pi]$,
- α_{21}, α_{31} - the two Majorana CP-violation phases.
- $\Delta m^2_{\odot} \equiv \Delta m^2_{21} \cong 7.6 \times 10^{-5}$ eV$^2 > 0$, $\sin^2\theta_{12} \cong 0.318$, $\cos 2\theta_{12} \gtrsim 0.24$ (3σ),
- $|\Delta m^2_{\rm atm}| \equiv |\Delta m^2_{31}| \cong 2.4 \times 10^{-3}$ eV^2, $\sin^2\theta_{23} \cong 0.5$,
- θ_{13} - the CHOOZ angle: $\sin^2\theta_{13} < 0.039$ (0.053) 2σ (3σ)

T. Schwetz et al., arXiv:0808.2016 (updated in 2010)

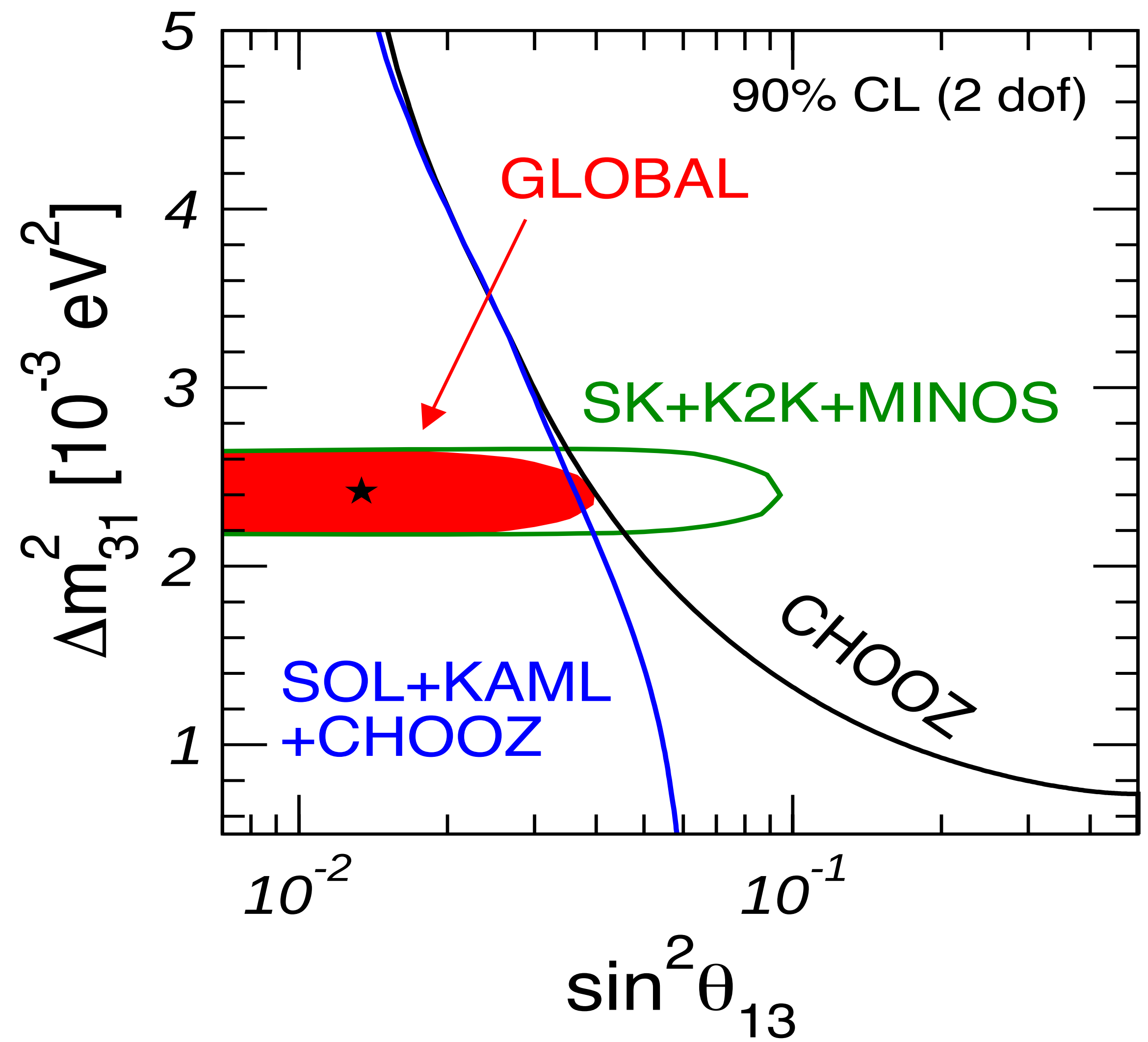

- $\sin^2\theta_{13} < 0.039$ (0.053) at 95% (99.73%) C.L.

T. Schwetz, M. Mezzetto, 2010

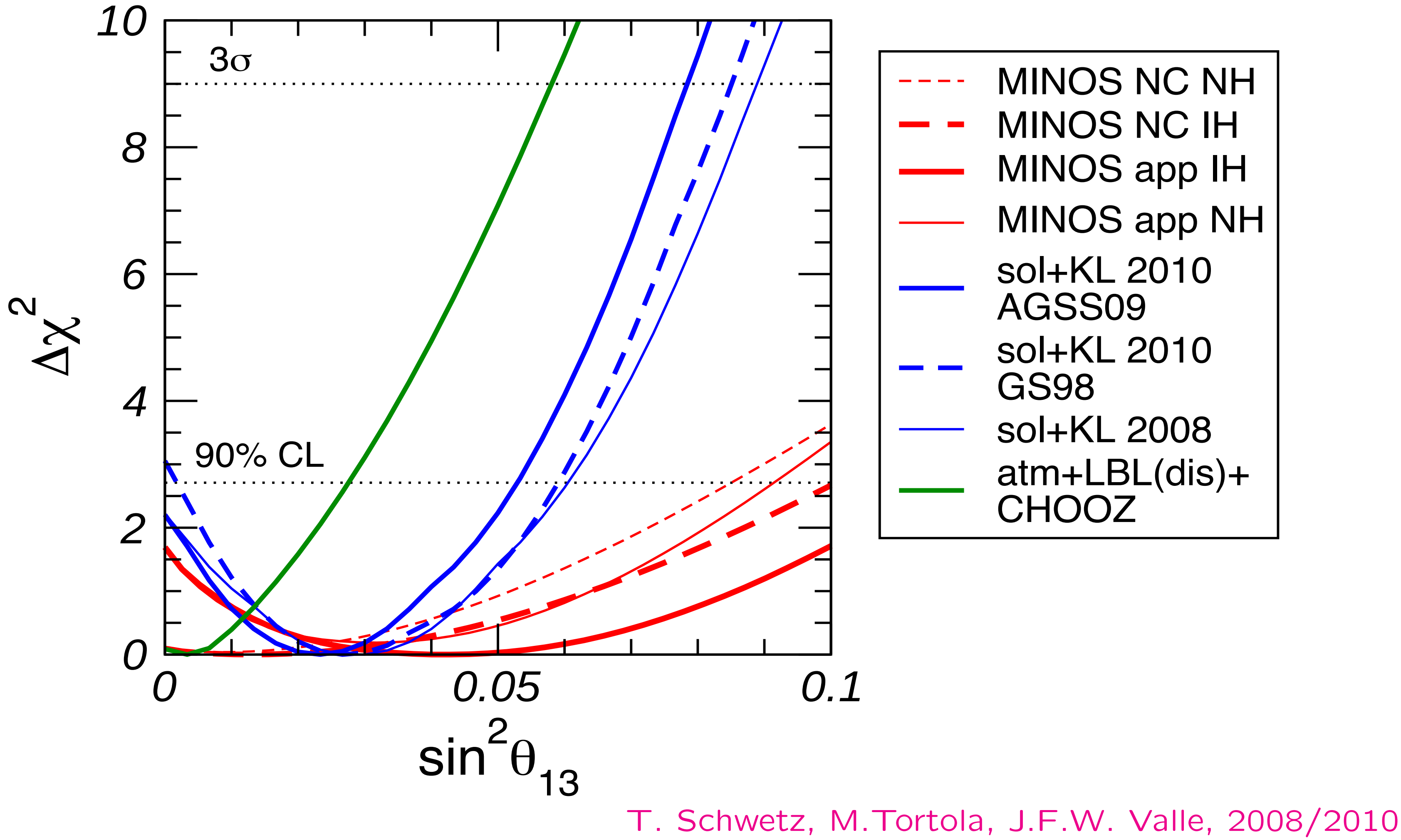
10
8
6
4
2
0
3σ
90% CL
0
0.05
0.1
$\Delta\chi^2$
$\sin^2\theta_{13}$
MINOS NC NH
MINOS NC IH
MINOS app IH
MINOS app NH
sol+KL 2010
AGSS09
sol+KL 2010
GS98
sol+KL 2008
atm+LBL(dis)+
CHOOZ
T. Schwetz, M.Tortola, J.F.W. Valle, 2008/2010

$$\sin^2\theta_{13} = 0.016 \pm 0.010, \ \sin\theta_{13} = (0.077 - 0.161)\,, \quad 1\sigma$$

E. Lisi *et al.*, arXiv:0806.2649

$$\sin^2\theta_{13} = 0.013^{+0.013}_{-0.009}\ , \ 1.3\sigma$$

T. Schwetz *et al.*, 2008/2010

Neutrino Oscillation Parameters

parameter	bf	1σ acc.	2σ range	3σ range
Δm^2_{21} $[10^{-5}\ \mathrm{eV}^2]$	7.59	3%	7.22 – 8.03	7.03 – 8.27
$\lvert\Delta m^2_{31}\rvert$ $[10^{-3}\ \mathrm{eV}^2]$	2.4	5%	2.18 – 2.64	2.07 – 2.75
$\sin^2\theta_{12}$	0.318	6%	0.29 – 0.36	0.27 – 0.38
$\sin^2\theta_{23}$	0.50	14%	0.39 – 0.63	0.36 – 0.67
$\sin^2\theta_{13}$	$0.013^{+0.013}_{-0.009}$	–	≤ 0.039	≤ 0.053

Best fit values (bf), relative accuracies at 1σ, and 2σ and 3σ allowed ranges of three-flavor neutrino oscillation parameters from a combined analysis of global data.

T. Schwetz, M. Tortola, J.W.F. Valle, 2008/2010

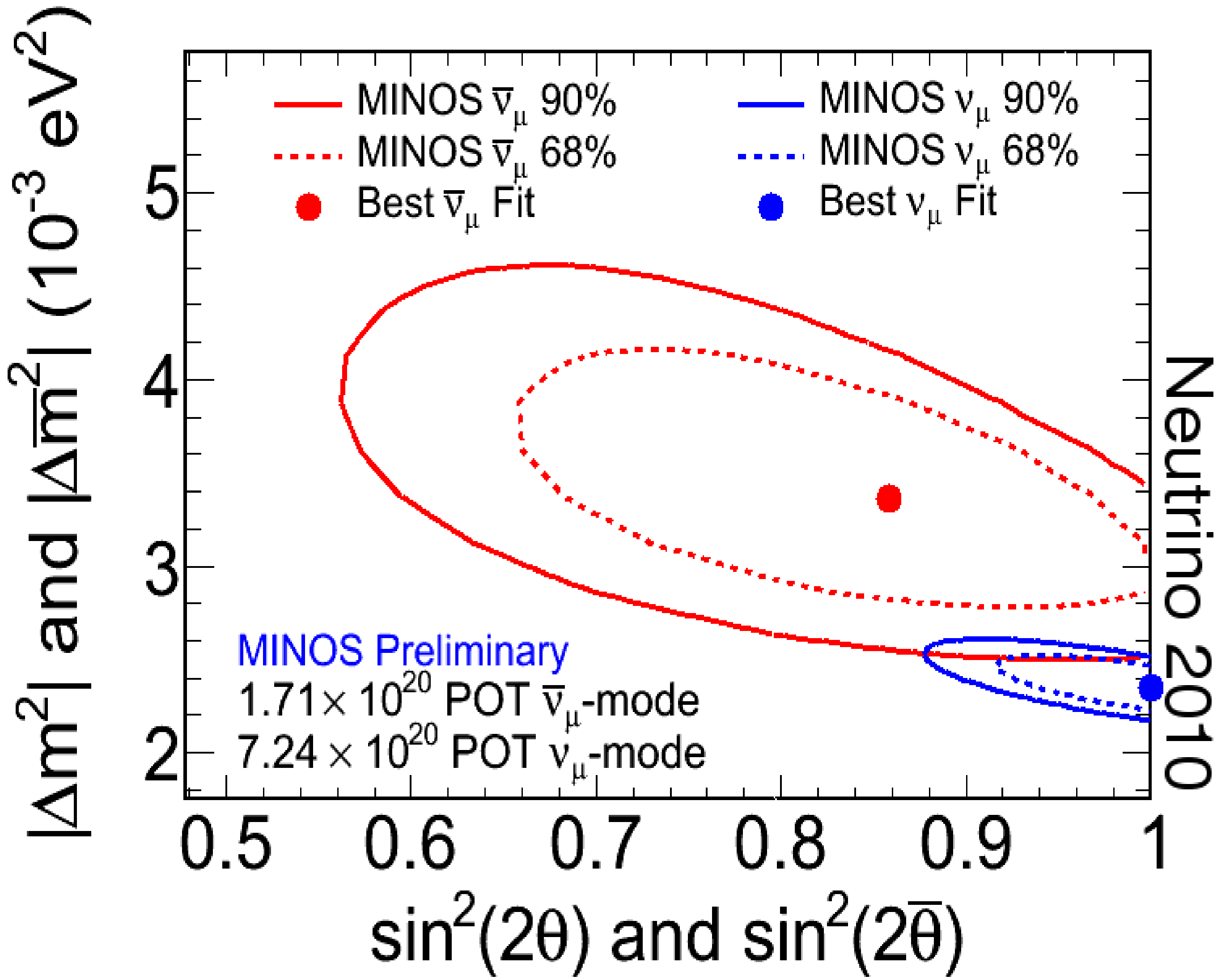

MINOS $\bar{\nu}_\mu$ 90%
MINOS $\bar{\nu}_\mu$ 68%
Best $\bar{\nu}_\mu$ Fit
MINOS ν_μ 90%
MINOS ν_μ 68%
Best ν_μ Fit
MINOS Preliminary
1.71×10^{20} POT $\bar{\nu}_\mu$-mode
7.24×10^{20} POT ν_μ-mode
Neutrino 2010
$|\Delta m^2|$ and $|\Delta \bar{m}^2|$ (10^{-3} eV^2)
$\sin^2(2\theta)$ and $\sin^2(2\bar{\theta})$
0.5
0.6
0.7
0.8
0.9
1
2
3
4
5

Search for CPT violation in atm. ν

Jun 2009

- Under the CPT theorem, P(ν→ ν) and P($\bar{\nu}$→$\bar{\nu}$) should be same.
- Test ν oscillation or $\bar{\nu}$ oscillation separately.

SK-I+II+III

Preliminary

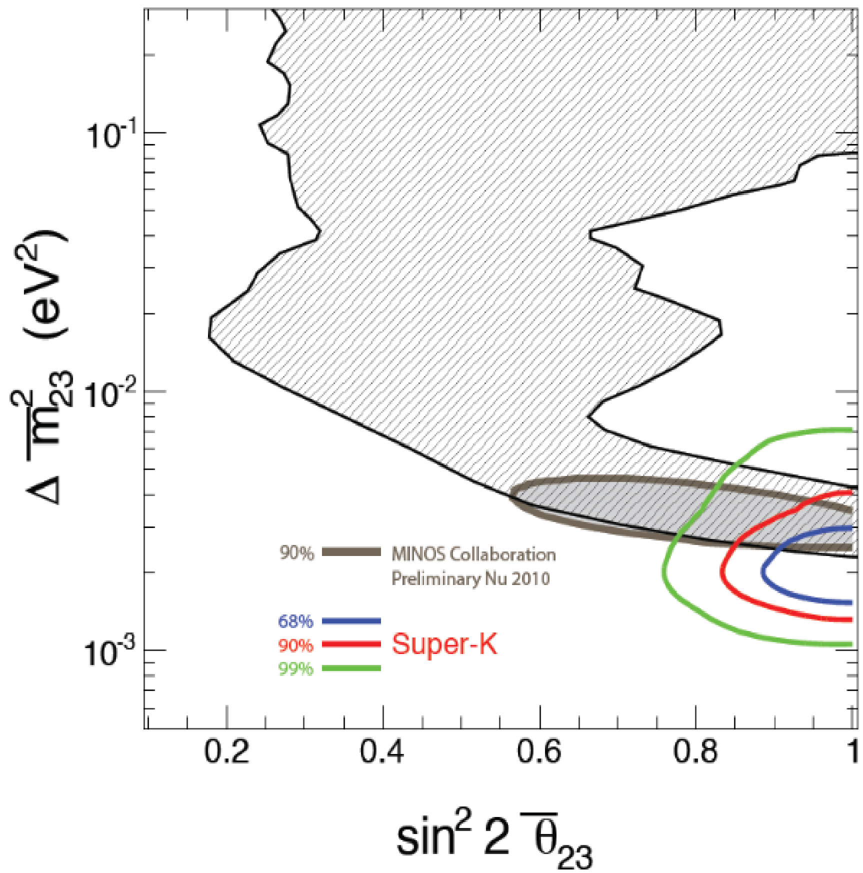

Neutrino:

$\Delta m_{23}^2 = 2.2\text{x}10^{-3}\text{eV}^2$

$\sin^2 2\theta_{23} = 1.0$

Anti-neutrino:

$\Delta \overline{m}_{23}^2 = 2.0\text{x}10^{-3}\text{eV}^2$

$\sin^2 2\overline{\theta}_{23} = 1.0$

No evidence for CPT violating oscillations is found

Poster-79 by Roger Wendell

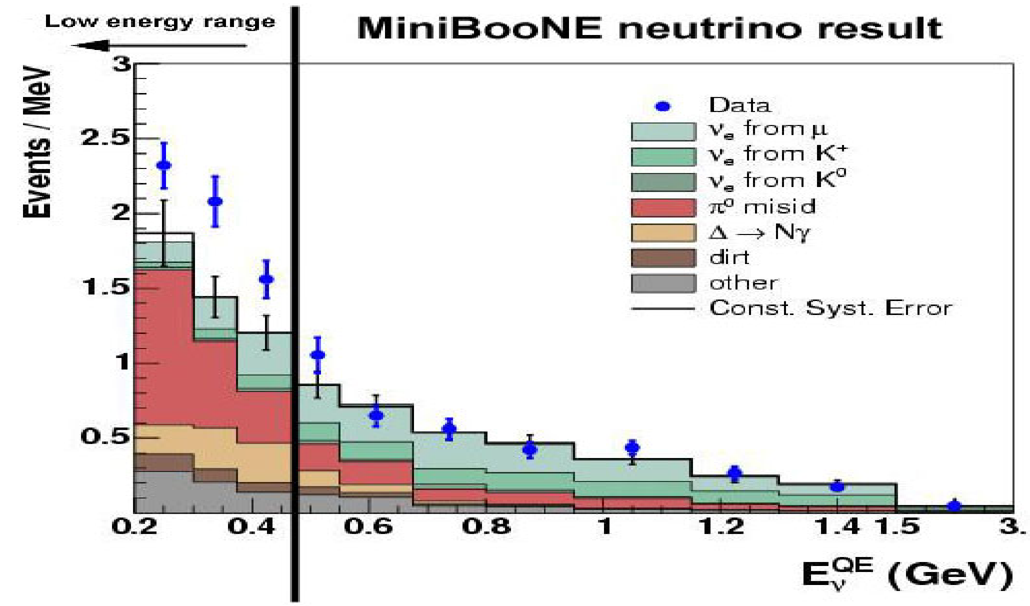
Low energy range
MiniBooNE neutrino result
Events / MeV
Data
ν_e from μ
ν_e from K^+
ν_e from K^0
π^0 misid
$\Delta \rightarrow N\gamma$
dirt
other
Const. Syst. Error
E_ν^{QE} (GeV)

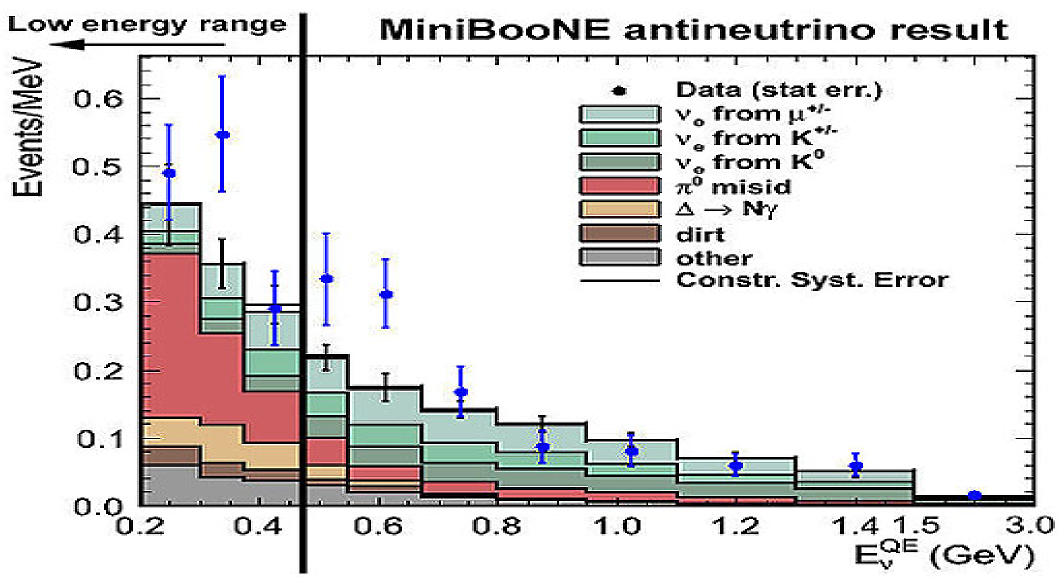
Low energy range
MiniBooNE antineutrino result
Events/MeV
Data (stat err.)
ν_e from $\mu^{+/-}$
ν_e from $K^{+/-}$
ν_e from K^0
π^0 misid
$\Delta \rightarrow N\gamma$
dirt
other
Constr. Syst. Error
E_ν^{QE} (GeV)

- $\text{sgn}(\Delta m^2_{\text{atm}}) = \text{sgn}(\Delta m^2_{31})$ not determined

$$\Delta m^2_{\text{atm}} \equiv \Delta m^2_{31} > 0, \quad \text{normal mass ordering}$$

$$\Delta m^2_{\text{atm}} \equiv \Delta m^2_{32} < 0, \quad \text{inverted mass ordering}$$

Convention: $m_1 < m_2 < m_3$ - NMO, $m_3 < m_1 < m_2$ - IMO

$$m_1 \ll m_2 < m_3, \qquad \text{NH},$$

$$m_3 \ll m_1 < m_2, \qquad \text{IH},$$

$$m_1 \cong m_2 \cong m_3, \; m^2_{1,2,3} >> \Delta m^2_{\text{atm}}, \; \text{QD}; \; m_j \gtrsim 0.10 \text{ eV}.$$

- Dirac phase δ: $\nu_l \leftrightarrow \nu_{l'}$, $\bar{\nu}_l \leftrightarrow \bar{\nu}_{l'}$, $l \neq l'$; $A^{(l,l')}_{\text{CP}} \propto J_{\text{CP}} \propto \sin\theta_{13} \sin\delta$
- Majorana phases α_{21}, α_{31}:
  - $\nu_l \leftrightarrow \nu_{l'}$, $\bar{\nu}_l \leftrightarrow \bar{\nu}_{l'}$ not sensitive;

S.M. Bilenky, J. Hosek, S.T.P.,1980;
P. Langacker, S.T.P., G. Steigman, S. Toshev, 1987

  - $\left| < m > \right|$ in $(\beta\beta)_{0\nu}$−decay depends on α_{21}, α_{31};
  - $\Gamma(\mu \rightarrow e + \gamma)$ etc. in SUSY theories depend on $\alpha_{21,31}$;
  - BAU, leptogenesis scenario: $\alpha_{21,31}$!

Comparison of hierarchies

May 2010

Best fit is in the inverted hierarchy case
Normal hierarchy (NH): χ^2_{min} = **469.94**/416dof
Inverted hierarchy (IH): χ^2_{min} = **468.34**/416dof

→ $\Delta\chi^2 = 1.6$

No significant difference

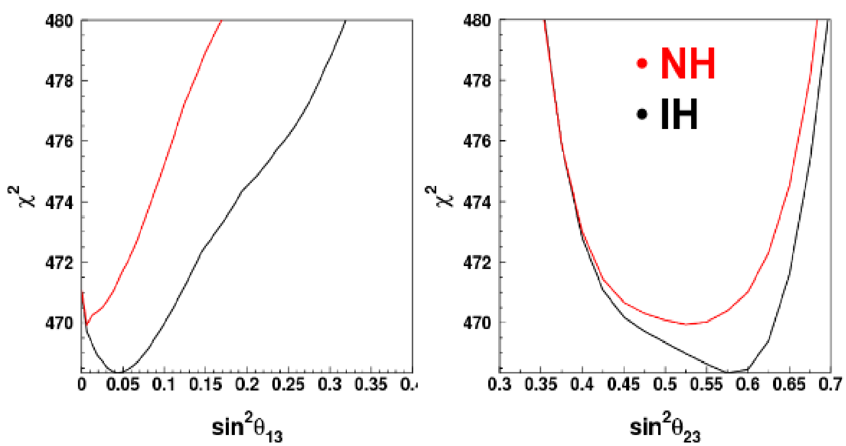

Multi-GeV samples tend to favor inverted hierarchy.

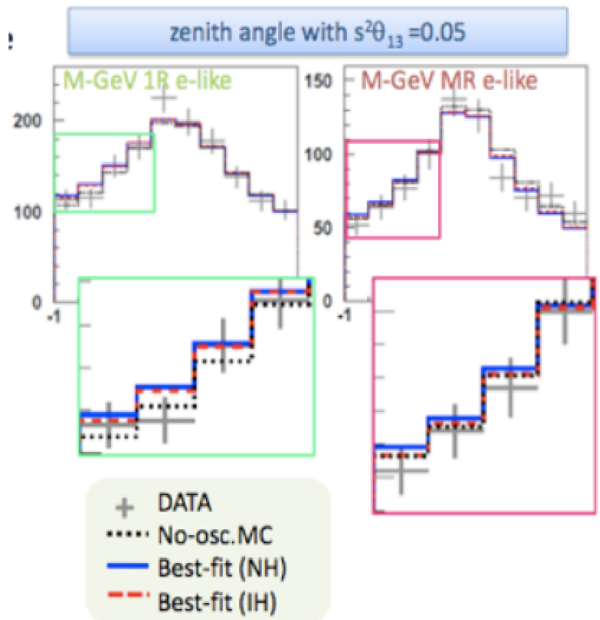

There are also some contributions from Multi-GeV μ-like samples favoring IH to NH.

Absolute Neutrino Mass Measurements

The Troitzk and Mainz ^{3}H β-decay experiments

$$m_{\nu_e} < 2.3 \text{ eV} \qquad (95\% \text{ C.L.})$$

There are prospects to reach sensitivity

$$\text{KATRIN}: \qquad m_{\nu_e} \sim 0.2 \text{ eV}$$

Cosmological and astrophysical data: the WMAP result combined with data from large scale structure surveys (2dFGRS, SDSS)

$$\sum_j m_j \equiv \Sigma < (0.4 - 1.4) \text{ eV}$$

The WMAP and future PLANCK experiments can be sensitive to

$$\sum_j m_j \cong 0.4 \text{ eV}$$

Data on weak lensing of galaxies by large scale structure, combined with data from the WMAP and PLANCK experiments may allow to determine

$$\sum_j m_j: \qquad \delta \cong 0.04 \text{ eV}.$$

Future Progress

• Determination of the nature - Dirac or Majorana, of ν_j .

• Determination of sgn($\Delta m^2_{\rm atm}$), type of $\nu-$ mass spectrum

$$m_1 \ll m_2 < m_3, \qquad \text{NH},$$

$$m_3 \ll m_1 < m_2, \qquad \text{IH},$$

$$m_1 \cong m_2 \cong m_3,\ m^2_{1,2,3} >> \Delta m^2_{\rm atm},\ \text{QD};\ m_j \gtrsim 0.10 \text{ eV}.$$

• Determining, or obtaining significant constraints on, the absolute scale of ν_j-masses, or min(m_j).

• Status of the CP-symmetry in the lepton sector: violated due to δ (Dirac), and/or due to α_{21}, α_{31} (Majorana)?

• Measurement of, or improving by at least a factor of (5 - 10) the existing upper limit on, $\sin^2\theta_{13}$.

• High precision determination of $\Delta m^2_{\odot}$, $\theta_{\odot}$, $\Delta m^2_{\rm atm}$, θ_{atm}.

• Searching for possible manifestations, other than ν_l-oscillations, of the non-conservation of L_l, $l = e, \mu, \tau$, such as $\mu \rightarrow e + \gamma$, $\tau \rightarrow \mu + \gamma$, etc. decays.

• Understanding at fundamental level the mechanism giving rise to the $\nu-$ masses and mixing and to the L_l-non-conservation. Includes understanding

– the origin of the observed patterns of ν-mixing and ν-masses ;

– the physical origin of CPV phases in $U_{\rm PMNS}$;

– Are the observed patterns of ν-mixing and of $\Delta m^2_{21,31}$ related to the existence of a new symmetry?

– Is there any relations between $q-$mixing and $\nu-$ mixing? Is $\theta_{12} + \theta_c = \pi/4$?

– Is $\theta_{23} = \pi/4$, or $\theta_{23} > \pi/4$ or else $\theta_{23} < \pi/4$?

– Is there any correlation between the values of CPV phases and of mixing angles in $U_{\rm PMNS}$?

• Progress in the theory of ν-mixing might lead to a better understanding of the origin of the BAU.

– Can the Majorana and/or Dirac CPVP in $U_{\rm PMNS}$ be the leptogenesis CPV parameters at the origin of BAU?

Instead of Conclusions

We are at the beginning of the Road...

Jacques would have liked the future exciting developments and would have made significant contributios at least to some of them.